UNIVERSITY OF TURKU

ELECTROCHEMICAL FABRICATION OF NANOCOMPOSITES TOWARDS SUSTAINABLE ENERGY APPLICATIONS

Milla Suominen

TURUN YLIOPISTON JULKAISUJA – ANNALES UNIVERSITATIS TURKUENSIS
SARJA - SER. AI - TOM. 601 | ASTRONOMICA - CHEMICA - PHYSICA - MATHEMATICA | TURKU 2019

UNIVERSITY OF TURKU

ELECTROCHEMICAL FABRICATION OF NANOCOMPOSITES TOWARDS SUSTAINABLE ENERGY APPLICATIONS

Milla Suominen

TURUN YLIOPISTON JULKAISUJA – ANNALES UNIVERSITATIS TURKUENSIS
SARJA - SER. AI - TOM. 601 | ASTRONOMICA - CHEMICA - PHYSICA - MATHEMATICA | TURKU 2019

University of Turku

Faculty of Science and Engineering
Department of Chemistry
Chemistry
Doctoral programme in Physical and Chemical Sciences

Supervised by

Professor Carita Kvarnström
Department of Chemistry
University of Turku
Turku, Finland

Adjunct Professor Pia Damlin
Department of Chemistry
University of Turku
Turku, Finland

Reviewed by

Professor Francesca Soavi
Department of Chemistry
Bologna University
Bologna, Italy

Professor Roberto M. Torresi
Department of Fundamental Chemistry
University of São Paulo
São Paulo, Brazil

Opponent

Professor Pedro Gómez-Romero
Catalan Institute of Nanoscience and Nanotechnology (ICN2)
Barcelona, Spain

The originality of this thesis has been checked in accordance with the University of Turku quality assurance system using the Turnitin Originality Check service.

ISBN 978-951-29-7554-9 (PRINT)
ISBN 978-951-29-7555-6 (PDF)
ISSN 0082-7002 (Print)
ISSN 2343-3175 (Online)
Grano Oy - Turku, Finland 2019

To my godchildren

TABLE OF CONTENTS

ACKNOWLEDGEMENTS

This work was conducted in the Laboratory of Materials Chemistry and Chemical Analysis in the research group of Materials Chemistry. First, I would like to thank Kiinteistösäätiö and the University of Turku Graduate School: Doctoral Programme in Physical and Chemical Sciences for supporting this project financially. Financial support in the form of travel grants from Kiinteistösäätiö, University of Turku, University of Turku Foundation and Fortum Foundation are also gratefully acknowledged as it has enabled the presentation of this work at following conferences: 67th Annual Meeting of the International Society of Electrochemistry (Hague, Netherlands), 7th International Symposium on Energy (Manchester, England), E-MRS Spring Meeting 2018 (Strasbourg, France), and 6th International Conference on Ionic Liquids for Electrochemical Devices (Rome, Italy).

I would like to thank the pre-examiners and opponent for taking time off your busy schedules to review my work. My deepest gratitude belongs to my supervisors, Prof. Kvarnström and Dr. Damlin, firstly for accepting me as their pupil, and secondly, for all the support, both intellectual and personal, I have received over the past years. I also thank my most important collaborators at Tampere University of Technology, Associate Prof. Sampo Tuukkanen and Dr. Suvi Lehtimäki. Without you this work would not be complete. My thanks also belong to Prof. Barbara Pałys at University of Warsaw, where I had the privilege to learn new electrochemistry and spectroscopy tricks. Thank you Dr. Anna Jabłońska and Mr. Mateusz Kasztelan for help during my visit and for showing me Polish traditions.

A big thanks to all the people working in the Laboratory of Materials Chemistry and Chemical Analysis and at the Department of Chemistry! Especially, I would like to thank my PhD student colleagues (Rahul, Sachin, Adefunke, Emilia, Isabella, Minnea, Ville, Lauri and Sergio, and Bhushan, Nianxing and Hellen who have already graduated) for making this fun from time to time. The work would also not be complete without the three wise wizards: technical wizard Mauri, IT wizard Kari, and reagent wizard Kirsi. Especially, Mauri is thanked for numerous cell designs.

To my families, both the one given to me in birth and the one that has formed during my studies, I owe thanks for all support. I thank my parents and my aunt Anja for giving me an upbringing which has made me the independent woman I am today, and my extended family on my father's side (especially Hantta and Mikko) for showing my international friends all the hospitality there can be in a Finnish home. Thank you Kermistit (especially Tapio, Maria and Kaisa) for being the best company during both undergraduate and graduate studies.

Final chapter is dedicated to the hairy men in my life. My four legged drooling companion Rosmo the corgi, who has become a kind of mascot in our laboratory, I thank for taking me to long walks where best ideas were born. And Pasi, who has evolved from a best friend and colleague to an indispensable companion, I thank for all the hugs during my moments of self-doubt.

Turku, January 2019
Milla Suominen

ABSTRACT

In the fight against climate change, effective energy storage applications are required to efficiently store the energy of renewable sources. Supercapacitors are one of the energy storage applications under vigorous research and development. Their ability to store a relatively large amount of energy and release it fast over millions of operating cycles has deemed these devices suitable for electric vehicles, for example. But current technology lacks in energy content which is why a novel category of supercapacitors, hybrid capacitors, has emerged. Hybrid capacitor can consist of a battery type electrode and a capacitor type electrode or both electrodes can be made of composite materials, which are materials composed of two or more individual components. Combining these components in right ratios gives the new composite material altered physico-chemical properties.

Several types of composites have been evaluated for use in supercapacitors, and one that has reached a lot of attention are composites between graphene and conducting polymers. The aim of this work has been to fabricate and thoroughly characterize these types of nanocomposites. In general, the large mechanically strong and well-conducting graphene should contribute to the cycling stability and power capability of the material while the conducting polymer should store and release large amount of energy. These nanocomposites can be fabricated by chemical and electrochemical approaches, which are presented in the literature background of this thesis. However, all of these fabrication approaches requires that both materials should be readily available as stable suspensions. The problems and solutions of producing graphene dispersions is therefore discussed in the literature review.

In the experimental part of this work a facile electrochemical approach is presented for the formation of composites between reduced graphene oxide and two different types of conducting polymers, poly(3,4-ethylenedioxythiophene) and polyazulene, in various ionic liquids. The approach used in this project is fast and takes advantage of the ionic liquids ability to disperse both the monomers and graphene oxide not to mention the improvement in electroactivity and cycling stability that is obtained by polymerizing conducting polymers in ionic liquids. The as-prepared composite materials have been thoroughly characterized by electrochemistry, spectroscopy, microscopy and spectroelectrochemistry.

TIIVISTELMÄ

Taistelussa ilmastonmuutosta vastaan tarvitaan tehokkaita energianvarastointisovelluksia, joilla voidaan tehokkaasti varastoida uusiutuvista energian lähteistä tuotettu energia. Superkondensaattorit ovat yksi energianvarastointisovelluksista, joita tutkitaan ja kehitetään tarmokkaasti. Niiden kyky vapauttaa suhteellisen suuri määrä energiaa nopeasti ja useiden miljoonien syklien ajan on ominaisuus, josta esimerkiksi sähköautot voivat hyötyä. Mutta kaupalliset sovellukset eivät pysty varastoimaan tarpeeksi energiaa minkä vuoksi on alettu kehittää hybridikondensaattoreita. Hybridikondensaattori voi koostua paristotyyppisestä elektrodista ja kondensaattorityyppisestä elektrodista tai molemmat elektrodit voivat koostua komposiittimateriaalista, jossa kaksi tai useampia materiaaleja on yhdistetty uudeksi materiaaliksi. Kun näitä materiaaleja yhdistetään oikeassa suhteessa toisiinsa, uuden komposiittimateriaalin ominaisuudet ovat huomattavasti erilaiset kuin yksittäisten komponenttien ominaisuudet.

Monenlaisten komposiittien ominaisuuksia superkondensaattoreissa on tutkittu ja yksi paljon huomiota saanut komposiittityyppi ovat grafeenin ja johdepolymeerien muodostamat materiaalit. Yleisesti ottaen mekaanisesti kestävä ja hyvin johtava grafeeni takaa pitkän eliniän ja nopean energian varastoinnin ja vapautuksen kun taas johdepolymeerin tehtävänä on varastoida suuri määrä energiaa. Näitä komposiitteja voidaan valmistaa useilla eri menetelmillä kuten kemiallisella polymerisaatiolla ja sähkökemiallisilla menetelmillä, joita käydään läpi tämän työn kirjallisuusosiossa. Kaikkien valmistusmenetelmien reunaehto kuitenkin on, että molempien materiaalien tulee muodostaa pysyviä seoksia useissa liuottimissa. Pysyvien grafeeniseosten aikaansaaminen on kuitenkin hankalaa ja mahdollisia keinoja pysyvien grafeeniseosten valmistamiseen käydään läpi työn kirjallisuusosiossa.

Työn kokeellisessa osiossa esitellään yksinkertainen sähkökemiallinen menetelmä, jossa valmistetaan komposiitteja pelkistetystä grafeenioksidista ja johdepolymeereista (poly(3,4-etyleenidioksitiofeeni) ja polyatsuleeni) ionisissa nesteissä. Tässä työssä käytetty menetelmä hyödyntää ionisten nesteiden kykyä liuottaa sekä johdepolymeerien monomeerejä että grafeenioksidia sekä niiden kykyä muodostaa sähkökemiallisesti aktiivisempia ja pysyvämpiä johdepolymeerikalvoja. Valmistetut komposiittimateriaalit on huolellisesti karakterisoitu sähkökemiallisin, spektroskooppisin, mikroskooppisin ja spektrosähkökemiallisin menetelmin.

LIST OF INCLUDED ORIGINAL PUBLICATIONS

The experimental part of this thesis is based on the following publications, which can be found reprinted with the permission from the copyright holders (Papers I-III and V: copyright © Elsevier) at the end of this thesis, and on some unpublished results. The publications are referred to in the text by their Roman numerals.

I. Damlin, P., **Suominen, M.**, Heinonen, M., and Kvarnström, C., Non-covalent modification of graphene sheets in PEDOT composite materials by ionic liquids, *Carbon* **93** (2015) 533-543.

II. **Suominen, M.**, Damlin, P., Granroth, S., and Kvarnström, C., Improved long term cycling of polyazulene/reduced graphene oxide composites fabricated in a choline based ionic liquid, *Carbon* **128** (2018) 205-214.

III. **Suominen, M.**, Damlin, P., and Kvarnström, C., Probing the interactions in composite of graphene oxide and polyazulene in ionic liquid by in situ spectroelectrochemistry, *Electrochim. Acta* **284** (2018) 168-176.

IV. **Suominen, M.**, Damlin, P., and Kvarnström, C., Electrolyte effects on formation and properties of PEDOT-graphene oxide composites, a manuscript submitted to *Electrochim. Acta*.

V. **Suominen, M.**, Lehtimäki, S., Yewale, R., Damlin, P., Tuukkanen, S., and Kvarnström, C., Electropolymerized polyazulene as active material in flexible supercapacitors, *J. Power Sources* **356** (2017) 181-190.

Contribution of the Author:

PAPER I: The Author executed the experimental work (excl. XPS and SEM) and helped to finalize the manuscript together with co-authors.

PAPER II: The Author planned the work together with supervisors, executed the experimental work (excl. XPS and SEM) and analyzed the data, wrote the first draft of the manuscript, and finalized it together with co-authors.

PAPER III-IV: The Author planned the work together with supervisors, executed the experimental work and analyzed the spectra, wrote the first draft of the manuscript, and finalized it together with co-authors.

Paper V: The Author planned the work together with supervisors and co-authors, executed the polymerization, 3-electrode measurements and structural characterization, wrote the first draft of the manuscript together with co-author and finalized it together with co-authors.

LIST OF OTHER RELATED PUBLICATIONS

Lehtimäki, S., Suominen, M., Damlin, P., Tuukkanen, S., Kvarnström, C., and Lupo, D., Preparation of Supercapacitors on Flexible Substrates with Electrodeposited PEDOT/Graphene Composites, *ACS Appl. Mater. Interfaces* **7** (2015) 22137-22147.

Viinikanoja, A., Kauppila, J., Damlin, P., Suominen, M., and Kvarnström, C., In situ FTIR and Raman spectroelectrochemical characterization of graphene oxide upon electrochemical reduction in organic solvents, *Phys. Chem. Chem. Phys.* **17** (2015) 12115-12123.

ABBREVIATIONS

AC	Activated carbon
ATR	Attenuated total reflection
aq	Aqueous
BF_4	Tetrafluoroborate
[Bmim]	1-butyl-3-methyl-imidazolium
[Bmp]	1-butyl-3-methyl-pyridinium
[Bmpy]	1-butyl-1-methyl-pyrrolidinium
C.B.	Conduction band
CCD	Charge-coupled device
CE	Counter electrode
CNT	Carbon nanotube
CP	Conducting polymer
CV	Cyclic voltammetry
EDOT	3,4-ethylenedioxy-thiophene
EDLC	Electrochemical double layer capacitor
EIS	Electrochemical impedance spectroscopy
[Emim]	1-ethyl-3-methyl-imidazolium
ErGO	Electrochemically reduced graphene oxide
ESR	Equivalent series resistance
EQCM	Electrochemical quartz crystal microbalance
FTIR	Fourier transformed infrared
FTO	Fluorine doped tin oxide
GCD	Galvanostatic charge/discharge
GD	Galvanostatic discharge
GO	Graphene oxide
[Hmim]	1-hexyl-3-methyl-imidazolium
IL	Ionic liquid
IR	Infrared
LbL	Layer-by-Layer
KF	Karl Fisher
PANi	Polyaniline
PAz	Polyazulene
PF_6	Hexafluorophosphate
PEDOT	Poly(3,4-ethylenedioxy-thiophene)
PPy	Polypyrrole
R&D	Research and Development
rGO	Reduced graphene oxide
RE	Reference electrode
SC	Supercapacitor
SEM	Scanning electron microscopy
SWCNTs	Single walled carbon nanotubes
TEM	Transmission electron microscopy
TfO	Triflate
TFSI	Bis(trifluoromethyl-sulfonyl)imide
TGA	Thermogravimetric analysis
UV-Vis	Ultraviolet-visible
V.B.	Valence band
VPP	Vapor phase polymerization
WE	Working electrode
XPS	X-ray photoelectron spectroscopy
XRD	X-ray diffraction

SYMBOLS

A	Electrode area
Ag/AgCl	Silver/Silver chloride
Ar	Argon
Au	Gold
C	Capacitance
d_p	Penetration depth
ΔE	Potential difference
E_{pa}	Oxidation peak potential
E_{pc}	Reduction peak potential
E_g	Band gap
E	Energy
E_0	Electric field strength
P	Power
Pt	Platinum
R	Resistance
R_{ct}	Charge transfer resistance
Si	Silicon
U_0	Cell voltage
ZnSe	Zinc selenide
ε_0	Vacuum permittivity
ε_r	Dielectric constant of the solvent
λ_{exc}	Excitation wavelength

1. INTRODUCTION

During recent years, the effects of climate change have become evident in our daily lives, and we are in a hurry to replace our current fossil fuel technologies with eco-friendlier alternatives. The means for harnessing renewable energy exists, but work must be done to efficiently store this energy so that it can be used when required. This should be done with a safe system available to everyone. Current technology for small electronics relies on Li-ions, but this technology can be dangerous due to exothermic reaction when the battery is damaged and, furthermore, Li is not the most abundant element. The market is also interested in bendable and wearable electronics. These are only some of the demands set for research and development (R&D) of tomorrow's energy storage devices.

Since the first patents in the 1960's, the energy storage device known as electrochemical double layer capacitor (EDLC) or supercapacitor (SC) has been the subject of vigorous R&D. SCs align between common batteries and capacitors in terms of operating performance; they can produce high amount of energy fast for thousands of times. SCs are applied in electric vehicles as complementary energy storage devices for batteries [1] and they can be applied in autonomous energy harvesting circuits for small electronics [2]. EDLCs can produce high amount of energy fast due to the physical energy storage mechanism based on the formation of an electrochemical double layer in the near vicinity of porous electrodes upon polarization of the electrodes (Fig. 1) [3]. Following equations help to elaborate R&D behind SCs:

$$Capacitance: \quad C = A\frac{\varepsilon_0 \varepsilon_r}{d} \tag{1.1}$$

$$Energy: \quad E = \frac{1}{2} C U_0^2 \tag{1.2}$$

$$Power: \quad P = \frac{U_0^2}{4R} \tag{1.3}$$

As electrode area is directly proportional to capacitance and energy, highly porous electrode materials are a necessity. Commercial EDLCs rely on activated carbon (AC), since it is readily available. ACs' high porosity ensures high capacitance while their chemical inertness enables thousands of operating cycles, but poor conductivity of ACs results in low power density since it is conversely proportional to the resistance. Carbon nanotubes (CNTs) [4] and graphene [5] have been proposed as substituents for ACs in EDLCs since they possess better conductivities. However, CNTs are expensive while graphene suffers from

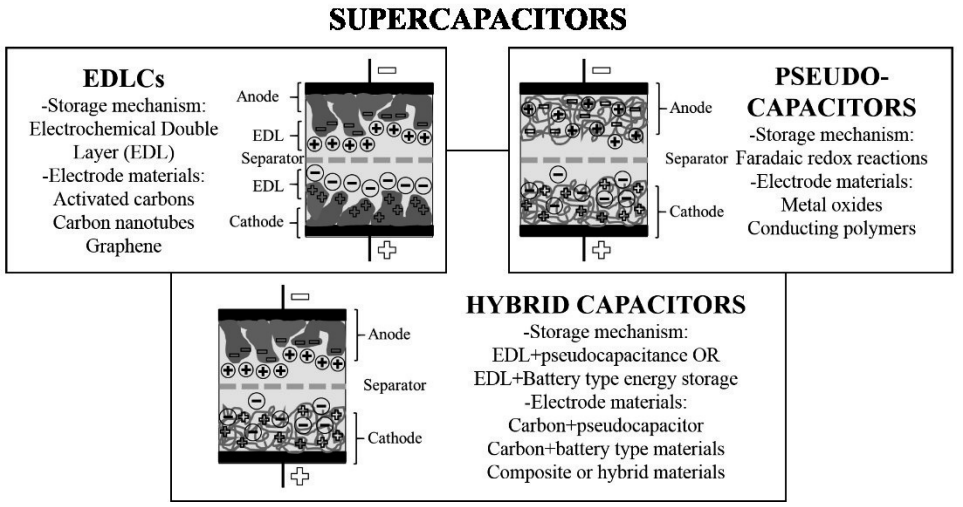

Figure 1. *A rough family tree of different types of SCs and their schematic cross sections.*

production issues. Electrochemical oxidation and reduction reactions of conducting polymers (CPs) and metal oxides are exploited in pseudocapacitors, introduced by Conway [6]. Pseudocapacitors are based on Faradaic charge transfer reactions taking place in the bulk electrode material which improves the energy content, but the advantage of extremely good long-term cycling stability is lost and, additionally, the slow kinetics of a redox reaction introduces a decrease in the important fast charging/discharging property.

It has been shown that it is favorable to implement both types of charge storage mechanisms to obtain better devices. This has emerged new type of SCs, hybrid capacitors, which cover a wide array of electrode materials and electrode configurations (Fig. 1). Hybrid capacitors can consist of two hybrid (composite) material electrodes, of a capacitor type carbon electrode (EDLC) combined with a pseudocapacitive electrode, or they can be a combination of a capacitor type electrode and a battery type electrode [7].

In the experimental part of this work we have aimed to fabricate and characterize nanocomposites of CPs and electrochemically reduced graphene oxide (ErGO) in ionic liquids (ILs) which could be utilized in hybrid capacitors (Papers I and II). The general hypothesis in fabricating these types of composites is that at certain ratios of the two materials, a synergy between the two components results in better electrode materials and ultimately improved device performance. Large sheets of ErGO are supposed to contribute as the mechanical support of the polymer material during long-term cycling, since degradation of pseudocapacitors is attributed to breaking of the polymer as a consequence of constant swelling and shrinking during doping and dedoping. The well-conducting graphene material should also contribute to

improved charging/discharging kinetics, while the polymer is expected to be the main contributor to high capacitance. By choosing electrochemistry as the material fabrication method, a facile technique for one-pot synthesis of electrodes is realized (Paper V), and by choosing ILs as our electrolyte, we have hoped to improve on the nanocomposite properties, because choosing the correct electrolyte for the device can also improve not only the energy content but also the cycling stability. ILs are a group of designer solvents that are aimed as electrolytes in energy storage devices because they possess low flammability and negligible vapor pressure, which are ideal properties for making safer devices compared to easily evaporating organic solvents, and good electrochemical stability enabling an increase in applied maximum voltages (U_0). ILs have also proven to improve the electroactivity and, most importantly, the cycling stability of CPs [8–10].

Firstly, background on the effects ILs have on the electrochemistry of CPs is given as it forms the basis of our fabrication approach. Since nanocomposite formation is best accomplished in solution phase, strategies to make stable graphene suspensions is discussed in the third chapter of the thesis. General approaches as well as the pros and cons of chemical and electrochemical nanocomposite formation are also presented in chapter three together with a short evaluation of the performance of CP based materials towards SC applications. Before outlining the main aims of the experimental work, charge carriers and electronic properties of CP based composites are discussed. Since doping changes the structure of CPs, the redox properties and the structural changes of CPs have been studied over the years with combined techniques known as *in situ* spectroelectrochemistry. The electron donating or withdrawing properties of the other component in CP based composites can have an effect on the charge carrier formation or conjugation length of the CP. Some *in situ* spectroelectrochemical studies have been performed on CNT based composites [11,12] and C_{60} fullerene type composites [13,14], but graphene based composites have not, to the best of our knowledge, been addressed although they have been extensively studied for a long time now. In the experimental part of this work (Papers III and IV), composite formation as well as the charge carriers and the electronic properties during doping of our nanocomposites has been studied by two *in situ* spectroelectrochemical techniques to elaborate the interactions between GO and CPs further.

2. CONDUCTING POLYMERS IN IONIC LIQUIDS

ILs are characterized as salts that melt at very low temperatures [15]. In practice, ILs should remain liquid preferably in room temperature or very close to room temperature, at least for most applications. The IL era properly began in the 1990's when ambient stable ILs were discovered [16], which consist of large (in)organic anions, such as tetrafluoroborate ($[BF_4]$), hexafluorophosphate ($[PF_6]$), bis(trifluoromethylsulfonylimide) ([TFSI]) and triflate ([TfO]), and of unsymmetrical organic cations, such as imidazolium, pyrrolidinium and pyridinium [17]. Initially promoted as "green alternative" to organic solvents, ILs have later revealed to produce toxic gases [18,19] not to mention their eco-toxicity and poor biodegradability [20–22], which is why ILs consisting of biomolecules, such as amino acids and choline [23–25], have been made to meet the demand of greenness. However, the biomolecule based ILs are still less used at least in electrochemistry which can be due to inferior properties or lack of commercially available choices. Today, also more specialized ILs, such as magnetic ILs [26], exist.

One property in common to all ILs is their intrinsic conductivity (0.1 – 20 mS cm^{-1}), since these solvents only consist of ions. They can have good electrochemical stability, depending on the ions they are made of, which allows the use of potential regions unattainable in conventional solvents. Impurities, water amongst the most common, however restricts these large electrochemical windows. Luckily, due to their negligible vapor pressures, ILs can be quite easily purified of water. These are the main reasons electrochemists adopted ILs early on. Electrochemistry in ILs is mostly hindered by their high viscosity which slows down mass transport. Lowering to the viscosity and an increase to the conductivity can be brought about by diluting them with organic solvents or by performing the measurements at elevated temperatures. The electrochemical techniques, which are applicable in ILs, include all the same methods that can be applied in organic electrolytes, but special care should be taken regarding the slow diffusion and Ohmic drop in certain conditions. [17]

One direction of applications is the use of ILs in the electrochemical polymerization and characterization of CPs, where ILs have been shown to have a myriad of fascinating effects. For example, the fabrication of some films is difficult in common solvents but electroactive films have been obtained in ILs [27,28]. CPs have managed to retain high interest since the year 2000 chemistry Nobel prize winners discovered in the late 1970's that simple polyacetylene can be made a metal-like conductor by exposure to iodine vapors [29]. The popularity of CPs is due to their versatility, simple manufacturing techniques and low cost. Decades of R&D has already resulted in some commercially available products, such as displays. The name conducting polymer refers to the conductivity of these types of polymers while

their other name, conjugated polymers, refers to their intrinsic conjugated structure which enables the conductivity. CPs consist of sp^2 hybridized carbons and the electrons in their p_z orbitals are delocalized over long ranges. However, CPs do not conduct electricity without the act of doping induced either by chemicals or, more commonly, by applying potential. Reduction (n-doping) or oxidation (p-doping) results in the insertion or removal, respectively, of electrons from the p_z orbital allowing movement of charge carriers in the polymer thus changing it from an insulator to semi-conductor or even metal-like conductor. Simultaneously, charge neutrality must be obeyed and doping of CPs is accompanied by the presence of dopants of opposite charge. The redox behavior of CPs can be simply monitored by cyclic voltammetry (CV) where typically broad peaks followed by current plateau is observed, and the peak currents vary linearly with the square root of scan rate due to diffusion limited reactions. [30]

CPs can be produced by chemical oxidative polymerization or electrochemical polymerization. They form through repeated radical cation formation, coupling and deprotonation, until at certain length the polymer precipitates from the solution or is attached to the electrode [30]. To the best of our knowledge, this mechanism is not changed in ILs [31], but ILs still affect especially the polymerization rate. Some works have reported that monomer oxidation takes place at lower potentials and that nucleation loop is missing in ILs due to improved stabilization of the radical cations in ILs [32]. Most works report on the change of deposition rate compared to organic solvents, and both slower and faster film formation has been explained by the high viscosity of ILs. An early report on the polymerization of pyrrole to polypyrrole (PPy) suggested that PPy polymerization rate is enhanced in certain ILs due the slow diffusion of reactive species to the electrode vicinity in higher viscosity medium [33,34], but in a later study, the polymerization of PPy was observed to be slower in some ILs [35]. Also, the polymerization of EDOT [36], aniline [34], thiophene, bithiophene and terthiophene [37], and azulene [32][V] was slowed down in higher viscosity IL. The differences in polymerization of poly(3-methylthiophene) in two pyrrolidinium based ILs was attributed to different conductivities and polarities of the two ILs [38]. If we follow the principle of Occam's razor, the simplest explanation is that the high viscosity of ILs slows down the diffusion of reactive species to the near vicinity of the electrode and thus, in general, slows down the deposition rate of CPs.

Another interesting aspect is that independent of faster or slower film formation, the films produced in ILs have superior performance in terms of electroactivity [32,34–36] and cycling stability [2,8–10,39–43]. Reasons for these improvements cannot be accounted for one property only. Firstly, polymerization in ILs naturally affects the morphology of CPs since their microstructure depends strongly on the polymerization environment. Again, both the formation of a denser film and a more

porous film are explained to lead to higher electroactivity. The former is defended by the fact that electronic charges can move more easily in a densely packed film while the second one by the easier movement of counter ions in the porous matrix. However, the necessity of film swelling is sometimes emphasized when denser film is formed [35,36]. Secondly, the improvements in electroactivity have been associated with higher amount of dopants present in ILs compared to conventional electrolytes [33,35], and thirdly, changes in the structure has also been proposed [14,35]. Formation of longer conjugation length has been suggested as the reason for improved electroactivity of polyazulene (PAz) [14]. Longer conjugation length was speculated to form due to the stabilization of ionic species in the IL which led to the formation of longer chains before they deposited on the electrode [32]. In this work, we discovered that using a very viscous IL might lead to shorter conjugation of PAz [V]. The mean conjugation length of PEDOT, however, should be similar independent of polymerization medium [44].

One of the most important properties of SCs is their long cycling life. CPs generally exhibit poor cycling stabilities in common solvents, which is a consequence of polymer degradation caused over time by constant stress directed to the polymer: during doping, counter ions and solvent molecules are taken into the film causing swelling while opposite behavior takes place during dedoping. Poor cycling stability of CPs in common solvents has also been attributed to over-oxidation of the polymer, nucleophilic attack of the solvent or degradation of the solvent [9,10,39]. Surprisingly, ILs have the ability to improve the long-term cycling stability of devices utilizing CPs [2,8,9,43]. This has been attributed to lower volume changes taking place during doping and dedoping in ILs which would result in less mechanical stress directed to the polymer. On the other hand, better electrochemical stability of ILs might also have an effect if solvent degradation is assumed as one contributor to poor cycling stability of CPs [9,10]. CPs have also been reported to endure higher applied potentials in ILs without significant degradation [45]. However, some exceptions exist: poly(3-(4-fluorophenyl)thiophene) polymerized and characterized in ILs had slower redox kinetics and poor electroactivity, which was attributed to the formation of a very dense film and gradual deswelling, respectively [46].

3. GRAPHENE-CONDUCTING POLYMER COMPOSITES

Composite material is, by definition, a material that consists of two or more distinguishable components that combined in suitable ratios give the new material significantly different physical and chemical properties from the individual materials. One of the best known examples of composites is concrete. In a nanocomposite, at least one of the components has dimensions of less than 100 nm or the differences between various phases of the material are in nanoscale order, and the idea is to gain similar or better improvements on the material properties with lower amount of filler material.

It seems only natural that the 2D wonder material graphene is applied in nanocomposites. Already in 2006 (only two years after the discovery of graphene), Nicholas Kotov wrote that graphene will be the cheaper option for CNTs in composites [47], but we are still waiting for the breakthrough. Since graphene's extraordinary properties [48] are associated with only single or few layers of the material, it is important to be able to produce single or few layered sheets in large quantities for fabricating low-cost commercial scale applications [49]. High quality graphene can be made through chemical vapor deposition (CVD) [50], epitaxial growth [51] and micromechanical exfoliation [52], but in low yields and with high cost. Colloidal suspensions are often the simplest and cheapest forms for up scaled production, though the quality of the graphene produced by exfoliating graphite in solvents is not as high [49].

3.1 Colloidal graphene suspensions

Preparing suspensions of graphene has caused some troubles in terms of obtaining high amounts of the material preferably as large individual sheets instead of as nanoplatelets. Since graphene consists only of carbon and hydrogen, and is thus non-polar, dispersing it in most known solvents usually requires the presence of surfactants. To this day, chemically modified graphene obtained by first oxidizing graphite with strong oxidants followed by reduction back to graphene-like structures remains the most used starting material for graphene-based applications. Actually, the use of graphite oxide in composite materials precedes the discovery of graphene [53]. Problems associated with using graphene oxide (GO) includes the requirement to further reduce it back to graphene-like since GO is non-conducting, the defects which remain in reduced GO (rGO) and make it less conducting than pristine graphene, and GOs' hydrophilic nature which makes it dispersible in water but not in organic solvents. Since homogeneous suspensions are a prerequisite in forming high quality nanocomposites, strategies to disperse graphene, GO and rGO are presented.

3.1.1 Non-covalent modifications

The easiest way of utilizing graphene would be to directly exfoliate graphite, since materials produced this way could be directly used without further modifications. One strategy is mechanical exfoliation by ball-milling or ultrasonication, but this requires careful matching of the solvent properties and the yields are quite low [54,55]. Usually, the best exfoliation results are accomplished only in the presence of surfactants, and the examples are numerous [56–63]. The analogy of graphene suspensions are dispersions of CNTs. Since CNTs can be considered as graphene sheets wrapped in the formation of a tube, they both possess similar large π-conjugated plane ideal for weak interactions with several surfactants, and often dispersing strategies developed for CNTs have been directly applied to graphene [54,60]. Interactions between the surfactants and graphene are π-π interactions with aromatic molecules and van der Waals forces with hydrophobic molecules.

Another strategy to exfoliate graphene without the presence of surfactants is electrochemical exfoliation, which is an intriguing choice as it may offer the advantage of controlling the end-product using a relatively mild and eco-friendly approach [64]. Electrochemically exfoliated graphene has already shown promise as electrodes in EDLCs [65–67]. Electrochemical exfoliation is divided into anodic and cathodic methods, first of which is more common and mostly conducted in aqueous electrolytes [68–70], and by adding sonication to the process, a more efficient exfoliation has been demonstrated [66]. However, these methods tend to introduce defects to the graphene structure due to the formation of extremely reactive radicals, which deteriorates the electronic properties of the exfoliated graphene. The process has been improved in the presence of antioxidants, for example [71]. Graphene can also be intentionally functionalized in the process: In a very recent work, graphite was exfoliated by an electrochemical method and simultaneously decorated covalently by diazonium salts which resulted in improved capacitive performance [72]. This is an interesting approach since it could diminish the amount of preparation steps required to obtain, for example, nanocomposites.

Electrochemical exfoliation has also been conducted in ILs, although, mixture of IL and water is required for the exfoliation to take place and the product is functionalized in the process [64,73]. Liu et al. [73] obtained an IL modified graphene which formed stable dispersions with many common organic solvents, and it was successfully incorporated in a polystyrene composite. They suggested that the mechanism of exfoliation includes the insertion of imidazolium radicals to the π-bonds of graphene, but this was criticized by Lu et al. [64] since Liu et al. did not take into consideration the radicals formed in the dissociation of water bound to take place at such over potentials. Lu et al. studied the electrochemical exfoliation further and suggested that water plays an important role as the hydroxyl and oxygen radicals

will oxidize the edge planes and facilitate the intercalation of the IL anion between the sheets [64]. They also concluded that changes in the ratio of IL to water results in different end-products from nanoribbons (high IL:water ratio) to carbon particles (low IL:water ratio). Electrochemically exfoliated graphene has improved the characteristics of an electrochromic application [74].

3.1.2 Covalent modifications

Covalently modified graphene materials offer a good platform for nanocomposite formation since the sheets are decorated with highly reactive functional groups, ideal for further reactions to take place. The best known covalent modification of graphene is the formation of GO. This is accomplished by first oxidizing graphite flakes with strong oxidants using methods originally developed by Brodie [75], Staudenmaier [76], or Hummers and Offeman [77], followed by sonication to separate the graphite oxide flakes to single or few layered GO. GO can be further modified back to graphene-like through myriad of reduction techniques [78–81] or the reactive oxygen functionalities can be further modified by covalently attaching desired molecules on them.

Although its structure remains a debate, GO sheets are believed to be decorated with carboxyl, hydroxyl and epoxy groups. All these groups can be further functionalized. Again, procedures developed for CNTs are sometimes applicable to GO [82]. In one of the first examples, graphite oxide was treated with isocyanates yielding a covalently modified material that could be dispersed in polar aprotic solvents [83] and further incorporated in a polystyrene composite, that showed sufficient conductivity for many electronic applications with record low percolation threshold [84]. Isocyanate attached to the carboxyl and hydroxyl groups of GO [83] while epoxide ring opening was expected to take place when GO was functionalized with octadecylamine [85] and polyallylamine [86]. The carboxyl groups have also been decorated with poly-(2-(dimethylamino)ethylmethacrylate) [87] and with a conducting polymer [88]. Actually, one approach to improve the nanocomposite formation between CPs and graphene towards SCs is to covalently graft the CPs to GO [89].

As the covalent modifications are difficult to remove and might not be advantageous in some applications, there are numerous attempts to disperse either GO in organic solvents or rGO in aqueous medium by non-covalent interactions. Although there are papers showing that GO [90] or rGO [91] could be dispersed as such, usually a surfactant is required to obtain practical concentrations. Interactions between the surfactants and GO or rGO are expected to be similar to those observed for graphene but the oxygen moieties that are present in both materials should contribute to additional weak interactions, such as hydrogen bonding or ionic interactions. For example, stable suspensions of rGO in water have been obtained in

the presence of poly(sodium 4-styrenesulfonate) [92], sodium dodecylbenzene sulfonate [93], and an amphiphilic molecule [94]. The fabrication of nanocomposites has also been eased by using inorganic metal oxide decorated graphene suspension as a precursor [95].

But to retain high conductivity in the final product, surfactants are also not always desirable, and it would seem that in composite fabrications GO is favored as starting material. ILs ability to disperse CNTs has been known for quite some time [96,97]. Therefore, it is not surprising that also GO and rGO can be dispersed in ILs at quite good yields [98–100]. There is some amount of debate as to why CNTs and graphenes form stable suspensions in ILs. The interactions between single walled carbon nanotubes (SWCNTs) and imidazolium based ILs should mainly be weak van der Waals interactions [97] but due to the extended π-bonding network of graphene and CNTs also π-π interactions and cation-π interactions have been suggested [98]. As will be discussed later, the role of water should also always be taken into consideration since complete removal of water from GO would appear to be very difficult. Naturally, the physico-chemical properties of ILs are also important contributors to stable suspensions, i.e. water miscibility or immiscibility mostly determined by the anion moiety of the IL. As is later shown, ILs constituting the [TFSI] anion, generally attributed to water immiscible ILs, do not usually form stable GO suspensions.

3.2 Composite fabrication methods

Strategies for fabricating nanocomposites can be categorized in many ways: according to the processes of synthesizing graphene [101] or by polymerization routes [102], for example. In this work, the fabrication approaches have been roughly divided into following categories according to the composite synthesis routes: (i) chemical approaches, (ii) electrochemical approaches, and (iii) miscellaneous approaches which include more sophisticated techniques such as hydrogels [103], Layer-by-Layer (LbL) assembly [53] and vapor phase polymerization (VPP) [104]. The electrochemical approaches also include partially electrochemical methods where parts of the process have been made chemically. The focus in this work has been to apply electrochemistry, but also the chemical approaches are presented since they constitute larger part of nanocomposite fabrication.

3.2.1 Chemical fabrication approaches

Chemical fabrication of CP/graphene nanocomposites is by far the most popular approach since these methods are usually simple and straightforward, and large amounts of composite can be produced. These approaches are named similarly to the approaches used for making composites of non-conducting polymers, and they

include solution mixing [105–107] and *in situ* polymerization [108–114]. In the former approach, the stable graphene, GO or rGO suspension and CP suspension are prepared separately, then mixed together, and the final product is washed and dried. In solution mixing, the polymer is expected to adsorb onto the graphene material with weak interactions. If GO has been used as filler material, an additional reduction step is needed, which is often also accomplished with chemical methods. Chemical reduction can, however, result in degradation of the polymer [115]. Solution mixing approach is less used than *in situ* polymerization where the chemical oxidative polymerization of the CP is performed in the graphene, GO [108,109,113,114] or rGO [111] suspension. The reduction of GO has been performed simultaneously [113] or after polymerization [109], again presenting a risk for polymer degradation. In this method, the CP is expected to polymerize on the graphene sheets, although many mechanisms may also compete affecting the final morphology and capacitive properties [114].

Nguyen and Yoon have compared chemical and electrochemical polymerization of CPs in terms of variables in the synthesis process, cost effectiveness, morphology control, reaction time, scalability and purity of the materials [102]. According to their results, chemical polymerization has less variables, lower cost and is easier to scale-up compared to electrochemical fabrication. It is possible to make inks for printing [116] or form composite papers [107] through chemical polymerization which are industrially desirable manufacturing techniques, but Yoon and Nguyen have left out environmental effects from their evaluation, for example. The road to the final electrode through chemical fabrication usually requires several washing steps, usually with organic solvents, and since a powder is obtained as product, additional polymer blends need to be added which can reduce the conductivity of the final electrode.

3.2.2 Electrochemical nanocomposite fabrication

The electrochemical approaches vary from polymerizing the CP on top the graphene-based material [117] to using GO as the dopant during the polymerization [118–127] and to simply hoping for the large sheets to be entrapped in the film during polymerization [128]. Partially electrochemical techniques have also been used, where electrochemistry has been applied for the formation of the electrodes after chemical composite fabrication [113] or the polymer is electrochemically formed on top of chemically prepared graphene-paper [129]. GO can be reduced before [125], after [120,124] or during [122] nanocomposite formation, and the most environmental friendly way of doing it is by applying cathodic potentials [115]. The possibility to reduce GO electrochemically even during film formation truly enables a one-pot synthesis of high quality electrodes for applications.

Naturally, the chosen approach should have a significant effect on the nanocomposite properties as varying degrees of interactions between the components should take place. The mechanism of composite formation must vary between the different approaches, but there are only few speculations on what happens during electrochemical polymerization of CP/graphene nanocomposites. In aqueous solutions, GO is expected to be partially deprotonated and possess a negative charge [130] which makes it the only counter anion balancing the cations during polymerization [121,124]. Increase in the pH of the polymerization dispersion has improved the composite formation since in low pH most carboxylic acid groups are expected to be protonated [115]. Deng et al. have proposed that during polymerization the radical cations of PPy are attracted to the basal planes of negatively charged GO followed by polymerization of pyrrole on top of GO [126]. Other studies have suggested that increasing the number of carboxylic groups on the basal plane of GO would result in improved synergy between GO and the CP since the CP would polymerize from the carboxylic groups [131]. There is also results that suggest ionic interactions between GO and PEDOT [127].

Electrochemical fabrication is usually criticized for its poor scalability though it beats the chemical fabrication in terms of material purity [102] and environmental friendliness since the materials can be directly applied to device substrates [2,132][V]. Another problem associated with electrochemical composite formation is the reproducibility. The amounts of both CP and graphene are easily controlled in a chemical approach, but when GO is used as a dopant, the amount of incorporated graphene cannot be controlled to similar extent as in the chemical techniques, although it is shown in [126] that as the amount of GO increases in the polymerization medium, it also increases in the film.

3.3 Comparison of nanocomposites

The important parameters studied of a material aimed at SCs are capacitance, rate capability and long-term cycling stability. The materials can be studied as such in 3-electrode setups, which gives preliminary information on the materials suitability towards SCs, but for more accurate knowledge of the properties, 2-electrode setups or, preferably, actual devices should be applied. There are numerous nanocomposites between graphene-based materials, CNTs, other carbon nanostructures, CPs, metal oxides, polyoxometalates, metal organic frameworks, biopolymers and non-conducting polymers aimed at SCs. Binary and, in increasing numbers, also tertiary nanocomposites have been reported. Table 1 lists the capacitance and capacitance retention values of some nanocomposites between CPs and carbon nanostructures. All these materials show promise towards SCs, but comparing them and putting them in rank order is difficult due to varying

measurement procedures, which has recently been criticized [133]. The values vary depending on the cell configuration, measurement technique, scan rate, electrolyte solution, potential range, and calculation method.

Some general trends can be cautiously outlined. Amongst CPs, polyaniline (PANi) is by far the most popular CP followed closely by PPy since they both exhibit high pseudocapacitance already as neat polymer films [134]. PANi and PPy based composites exhibit some of the highest capacitance values. Chemically produced materials have higher capacitances compared to electrochemically produced films, since the amount of material produced is substantially smaller in the latter technique. In electrochemical fabrication, the amount of material deposited is also of huge influence on the reported values [127]. In general, the capacitance tends to increase when the carbon nanomaterial is incorporated or when GO is reduced, but this is not always the case [128,135]. The increase in the electroactivity after composite formation is often attributed to synergy between the carbon material and the conducting polymer. For example, the formation of special charge-transfer complexes between the CP and graphene material has been explained as the basis for the improvements [112]. But some studies attribute the improved capacitance values to increased area.

Stability of EDLCs is often studied by voltage floating tests [136], but to the best of my knowledge, pseudocapacitors are still mostly tested by cycling methods. Amongst the studied CPs, PEDOT shows best tolerance towards long-term cycling while PANi has been reported to be the poorest CP in this parameter. Some of the highest improvements would appear to be reported exactly for PANi-based composites, with some exceptions [124], while very moderate improvements are brought to PEDOT. The required mechanical stability to improve the long-term cycling can also be brought about by incorporating a non-conducting polymer or biopolymer with the CP. This can decrease the conductivity, but it would appear that the use of cellulose shows very good promise in improving the long term cycling stability of PPy [137,138]. Despite big effort, the cycling stability of CP based materials has not been improved to the same level that is exhibited by other materials applied in SCs which has made them a less interesting electrode material [139].

Table 1. *Capacitances (C) and capacitance retentions (C_{ret}) of some films aimed at SCs. Symbols are as follows: GD, galvanostatic discharge; CV, cyclic voltammetry; EIS, impedance; [a], 2-electrode cell; [b], 3-electrode cell.*

Fabrication method	**Material**	**Scan rate (Method)**	**C**	**C_{ret} (No. of cycles)**	**REF**
in situ chemical polymeri-zation	PPy/MWCNT	*2 mA (GD)[a]*	*200 F/g*	-	[140]
	PANi/MWCNT		*360 F/g*		
	PEDOT/MWCNT		*120 F/g*		[141]
	PANi	*0.2 A/g (GD)[a]*	*300 F/g*	*74 % (2000)*	[114]
	PANi/GO		*555 F/g*	*92 % (2000)*	
	PANi	*0.2 A/g (GD)[b]*	*264 F/g*	*43 % (500)*	[110]
	PANi/rGO		*526 F/g*	*74 % (500)*	
	PPy/Cellulose/GO	*0.2 A/g (GD)[a]*	*244 F/g 198 F/cm^3*	*85 % (16000)*	[138]
	PPy/Cellulose	*33 A/g (GD)[a]*	*127 F/g 122 F/cm^3*	*93 % (5000)*	[142]
	SR-PE$_2$/CNT-T	*20 mV/s (CV)[a]*	*8 F/g 45 F/cm^2*	*83 % (10000)*	[133]
Solution mixing	PPy NPs/ErGO	*0.2 mA/cm^2 (GD)[a]*	*110 F/g 216 F/cm^2*	*87 % (5000)*	[107]
	PANi	*0.3 A/g (GD)[a]*	*214 F/g 116 F/cm^3*	*71 % (800)*	[105]
	PANi/rGO		*210 F/g 160 F/cm^3*	*79 % (800)*	
Electro-chemical	PANi	*0.5 A/g (GD)[a]*	*276 F/g*	*55 % (1000)*	[113]
	PANi/rGO		*384 F/g*	*84 % (1000)*	
	PEDOT	*10 mV/s (CV)[a]*	*59.1 F/cm^2*	-	[131]
	PEDOT/GO		*75.6 F/cm^2*	*95.7 % (5000)*	
	PEDOT/CGO		*90.9 F/cm^2*	*99.6 % (5000)*	
	PPy	*0.5 A/g (GD)[b]*	*147 F/g*	*74 % (800)*	[119]
	PPy/SG		*285 F/g*	*92 % (800)*	
	PANi	*EIS[b]*	*52.2 mF/cm^2*	*94 % (10000)*	[124]
	PANi/ErGO		*77.2 mF/cm^2*	*90 % (3000)*	
	PEDOT/ErGO	*EIS[b]*	*19.3 mF/cm^2*	-	[115]
	PEDOT/rGO	*EIS[b]*	*12.2 mF/cm^2*	*87 % (3000)*	[125]
	PEDOT/PSS	*0.1 V/s (CV)[b]*	*21.6 mF/cm^2*	*89 % (3000)*	[143]
	PEDOT/GO		*17.6 mF/cm^2*	*90 % (3000)*	
	PEDOT/rGO		*22.5 mF/cm^2*	*86 % (3000)*	
	PEDOT	*(GD)[a]*	*14 mF/cm^2*	*93.1 % (2000)*	[132]
	PEDOT/GO		*14 mF/cm^2*	*94.6 % (2000)*	
	PEDOT/ErGO		*18 mF/cm^2*	*93.2 % (2000)*	
	PAz	*(GD)[a]*	*27 mF/cm^2*	-	[V]
	PAz	*20 mV/s (CV)[b]*	*55 mF/cm^2*	*91 % (1200)*	[II]
	PAz/GO		*130 mF/cm^2*	*93 % (1200)*	

As was already mentioned and can be deduced from Table 1, the research around CP pseudocapacitors revolves around PANi, PPy and PEDOT. Reynold's group has introduced dioxythiophene derivatives to the competition that are easy to process [133], and naturally other thiophenes have also been studied [38]. Azulene is characterized as a non-benzenoid isomer of naphthalene, which due to the fused electron poor and electron rich seven membered ring and five membered ring, respectively, has a high dipole and is thus an interesting building block for many organic electronics devices. The ability to polymerize azulene to form polyazulene (PAz) is also not news, but for some reasons PAz has not provoked the same amount of interest that the monomer it consists of has. One reason could be that it is very difficult to polymerize it chemically. One successful case has required the use of a dibromo derivative of azulene to get the polymerization to take place in the desired 1- and 3-positions of the five membered ring and harsh reaction conditions, but the final product has exhibited quite low conductivity of 1.22 S cm^{-1} [144]. Electrochemical polymerization of azulene is a relatively simple process and yields films with better conducting properties [145]. Another reason could be its sensitivity to water or the high price tag on the monomer. Despite these issues, electrochemically produced PAz has high specific capacitance of 400 F g^{-1} [146]. The specific capacitance of PANi is expected to be only 130 F g^{-1} higher than the specific capacitance of PAz [134]. This has recently aroused more work on PAz, and especially the focus has been on applying PAz in specific applications, such as in solid-state ion selective electrodes [147]. Inspired by this, and by the knowledge that ILs can have a significant effect on the electroactivity of PAz [32], we studied the capacitive properties further in ILs in Paper V. The areal capacitance of our asymmetric PAz SCs gives similar or slightly higher values compared to PEDOT based materials (Table 1).

4. SPECTROELECTROCHEMISTRY OF COMPOSITES

CPs consist of extended π-bonding systems and, as a result of doping, they change from neutral form to conducting form. This induces both electronic and structural changes in the CPs that are visible in the UV-Vis-NIR and mid-IR regions [148,149]. Therefore, *in situ* spectroelectrochemistry is a powerful tool in determining important properties of CPs as these techniques combine the study of redox properties with the structure of the polymer. The transition from the valence band (V.B.) to conduction band (C.B.) (π-π* transition, Scheme 1.) usually lies in the visible part of the spectrum, and it gives an estimate of the band gap (E_g) [148]. The position of the π-π* transition related band is dependent on the conjugation length of the CP and on the delocalization of the π electrons [148,150]. Oxidation of CPs leads to the formation of polycations in the form of polarons and bipolarons for thiophenes (Scheme 1.) [151] and polarons and polaron pairs for PAz (Scheme 2.) [150,152] accompanied by the insertion of counter anions to compensate the formed positive charges. The formation of the charged species induces a change from a benzenoid structure to a quinoid structure, which is visible in vibrational spectra [149], whereas in the electronic spectra bleaching of the π-π* transition band is accompanied by the appearance of novel absorption bands originating from the free charge carriers [148].

The nature of CPs has been verified by several *in situ* spectroelectrochemical techniques over the past couple decades [44,150,152–155]. Additional dopants or changing the polymerization parameters [155] can affect the structure or electronic properties of CPs, which can be observed as changes in the positions of their characteristic doping induced bands. Although some of these changes can be deduced from CVs only, recording the spectra simultaneously might give a more

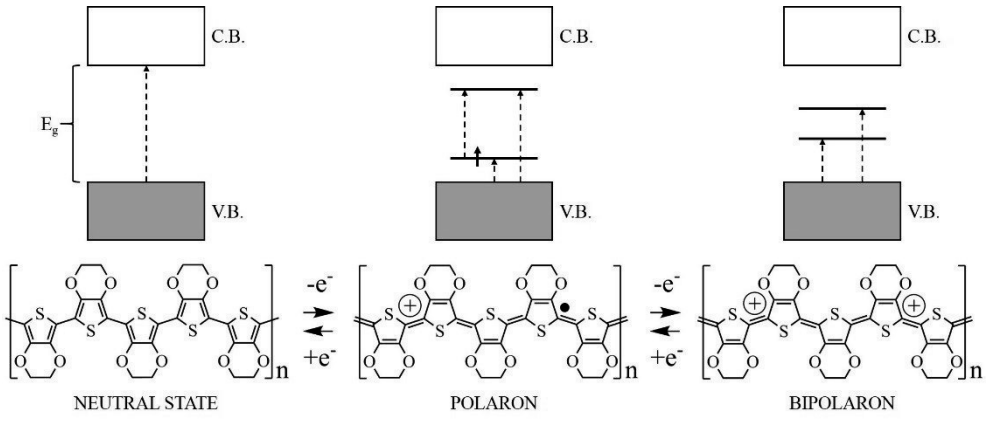

Scheme 1. *Band diagrams and proposed structures of polaron and bipolaron charge carriers in PEDOT*

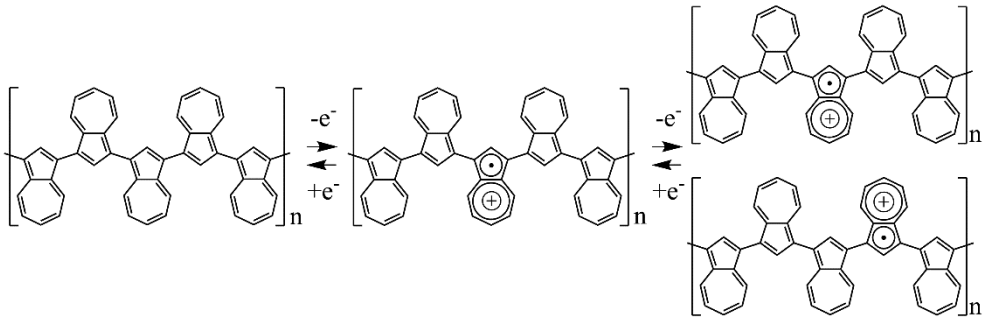

Scheme 2.*Proposed structures of polaron and polaron pair charge carriers in PAz. [III]*

detailed descriptions on the changes that take place. Therefore, many co-polymers or composites of conducting polymers have also been studied with *in situ* techniques. For example, PEDOT behaves similarly in common organic solvents and in ILs [44] but bilayers of PEDOT and C_{60} fullerene become conducting at lower potentials compared to a neat polymer film due to the electron withdrawing characteristics of the fullerene [13]. TiO_2 also has a tendency to accept electrons which resulted in a significant shift of PAz's electronic absorption to lower energies [156]. In composites of C_{60} and PAz, the conjugation length of the polymer became shorter in the presence of fullerene [14,32]. A donor-acceptor type layer of PAz and an n-type polymer revealed charge trapping during n-doping of the composite layers [157]. More recently, the charging mechanism of PPy/lignin composite aimed at energy storage applications [158] was determined by *in situ* spectroelectrochemistry [159].

The study of CP/graphene nanocomposites has focused on their electrochemical performance and composition. Especially when GO is used as dopant during the electrochemical fabrication of composites or when CPs are chemically polymerized or grafted onto GO or rGO, changes in the conjugation or electronic properties might take place. GO has been characterized as an electron withdrawing material [112], which should be seen through *in situ* analysis. Formation of composites between CPs and CNTs has been shown to affect the doping behavior of the nanotubes [11,12]. In a work by Yang et al. [120], the *in situ* UV-Vis spectra of a PPy/GO composite was recorded but it was interpreted only in terms of GO reduction, and the effects on polymer properties was not addressed. In addition to giving vital information on material characteristics, *in situ* spectroelectrochemistry has been applied on studying the charging mechanisms of EDLCs [160] and to determining the electrochemical stabilities of electrolytes in a more precise manner [14].

5. MAIN AIMS OF THE EXPERIMENTAL WORK

Main aim of this thesis project was to fabricate composites of conducting polymers and electrochemically reduced graphene oxide in ionic liquids, and to study their performance towards supercapacitor applications. Electrochemistry was our method of choice for the composite fabrication since it offers possibilities to control the film formation and it also enables a relatively mild route from poorly conducting GO to better conducting ErGO. Additionally, by electrochemical fabrication method, the film is formed directly on a conducting substrate, ready for end-use applications, without the need for further modification steps as is the case with chemically fabricated materials. ILs were chosen as the solvent medium due to their good properties in electrochemistry, i.e. broad electrochemical stability, and especially in electropolymerization of conducting polymer films, ILs have proven their worth for producing films of higher electroactivity. The additional benefit of using ILs is that both GO and the monomers could be dispersed into ILs in practical concentrations. The aim was also to study these composite materials by *in situ* spectroelectrochemistry to gain deeper insight into the properties of these types of nanocomposites.

In **Paper I**, a protocol for dispersing GO in imidazolium-based ILs was established and PEDOT/ErGO composites were polymerized directly from GO/IL dispersions in two ILs constituting different cations. In **Paper II**, GO was dispersed in various other ILs, this time constituting various cations and anions with very different physico-chemical properties, and PAz/ErGO composites were successfully fabricated in GO/[Choline][TFSI] dispersions. The composition and electrochemical behavior of PAz/ErGO composites were studied in **Paper II** and compared to PAz properties while the same properties were determined for PEDOT/ErGO composites in **Paper I**. **Papers III** and **IV** focus on understanding the underlying electronic properties as well as charge carrier formation of PAz/GO and PEDOT/GO composites, respectively. Additionally, in **Paper IV** the composite formation and electrochemical properties are compared between different electrolyte systems to gain deeper understanding of the interactions between GO and CPs. Apart from the other papers, in **Paper V** the capacitive behavior of neat PAz films was studied in different ILs and the performance of bendable symmetric and asymmetric PAz supercapacitors was determined for the first time.

6. SUMMARY OF EXPERIMENTAL TECHNIQUES

6.1 Dispersing graphene oxide in ionic liquids

GO was prepared by a modified Hummers method [161] according to a protocol summarized in Paper I. Stable dispersions of GO in ILs was obtained according to [98] by mixing desired volumes of GO aqueous solution with IL followed by ultrasonication and drying procedure, where the dispersions were first dried with rotary evaporator at 45 °C for 4 h followed by further 4 h in 45 °C vacuum oven (Memmert). Using low temperature was necessary to avoid thermal reduction of GO, and the ultrasonication before drying ensured that the GO sheets were well separated for efficient removal of water. The as-prepared GO/IL dispersions were analyzed by Karl-Fisher (KF) titration, thermogravimetric analysis (TGA), and FTIR and UV-Vis spectroscopies. The concentration of GO in the dispersions was determined with UV-Vis spectroscopy from the intensity of the shoulder at 300 nm using an absorption coefficient of 18.3 mL mg^{-1} cm^{-1}.

Upon adding GO(aq) to ILs incorporating the hydrophobic [TFSI] anion, instant agglomeration of GO was observed. The tested cations were 1-ethyl-3-methylimidazolium ([Emim]), 1-butyl-1-methylpyrrolidinium ([Bmpy]) and 1-butyl-3-methylpyridinium ([Bmp]). Even prolonged heating at 100 °C did not produce homogeneous dispersions in these [TFSI]-based ILs. To our surprise, a stable dispersion was obtained in a choline-based IL incorporating the [TFSI] anion, although the dispersions were homogeneous only after drying (Fig. 2a-c). Mixing and demixing behavior of a mixture of [Choline][TFSI] and water as a function of temperature has been observed previously [162]. Also, in 1-hexyl-3-methylimidazolium tetrafluoroborate ([Hmim][BF_4]) a phase separation was observed directly after adding GO(aq), which can be seen in Fig. 2d, where a layer of water is observed on top of the dispersion with 2 mg mL^{-1} concentration of GO. In water miscible ILs 1-butyl-3-methylimidazolium tetrafluoroborate ([Bmim][BF_4]), 1-butyl-3-methylimidazolium triflate ([Bmim][TfO]), and 1-butyl-3-methylpyridinium triflate ([Bmp][TfO]) light brown and homogeneous GO dispersions were obtained directly after mechanical mixing of GO(aq) and IL (Fig. 2e). All dispersions showed good stability over a longer period of time, although freshly prepared dispersions were used for composite film fabrication.

The removal of water was verified by KF titration, TGA, and IR spectroscopy by the disappearance of the characteristic broad OH stretching vibration at 3400 cm^{-1} (Fig. 3a-b). However, especially in [Hmim][BF_4], two bands at 3635 cm^{-1} and 3558 cm^{-1} would sometimes remain in the IR spectra of the dispersions after drying (Fig. 3a). These bands originate from “free” water molecules interacting with the anion through hydrogen bonding in a symmetric complex [163]. Further drying was

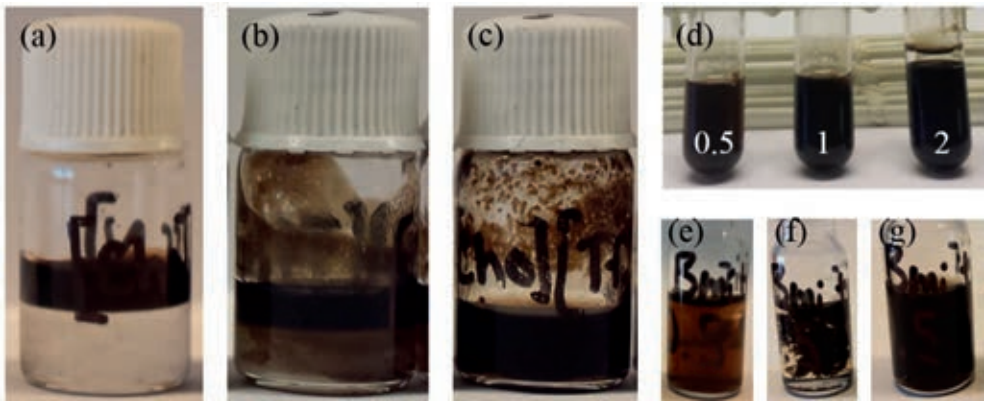

Figure 2. *(a-c) GO in [Choline][TFSI] (a) directly after combining the two solutions, (b) after overnight stirring and 15 min ultrasonication, and (c) after drying 4 h in 45 °C vacuum oven. [II] (d) Different concentrations of GO (mg mL^{-1}) in [Hmim][BF_4] after ultrasonication. (e) 0.5 mg mL^{-1} GO in [Bmim][TfO]. (f-g) Solvothermally reduced GO (150 °C for 4 h) in [Bmim][TfO] (f) directly after the procedure, and (g) after ultrasonication.*

applied, if these signals were observed. Also, both KF titration and TGA analysis suggested that certain amount of water is still present in the GO/IL dispersions after drying. Complete removal of water from GO seems somewhat impossible, and it is possible that some amount of water is actually required to obtain stable suspensions of GO in other media than water.

The UV-Vis spectrum of GO (Fig. 3c) presents an absorption at 231 nm attributed to the π-π* transitions of aromatic C-C bonds of the ketones or dienes, a broad shoulder at 300 nm attributed to the n-π* transitions due to the presence of C=O linkages, and a featureless absorption tail (Paper I). Upon reducing GO, the absorption at 231 nm gradually shifts to 270 nm while the shoulder at 300 nm vanishes and the absorption tail intensity increases as the conducting π network is restored [130]. The UV-Vis spectra of different GO/IL dispersions with varying GO concentrations are shown in Fig. 3c, and it shows that during solvent exchange and drying in low temperatures any significant conversion of functional groups did not take place in any of the applied ILs since GO features are present (Paper I). Some GO/IL dispersions were subjected to elevated temperatures in vacuum oven. The lowest concentration dispersions (0.5 mg mL^{-1}) in [Bmim][TfO] and [Bmp][TfO] showed agglomeration after 4 h at 150 °C (Fig. 2f) and a distinct color change from light brown to black can be observed. Similar color changes were observed for other dispersions as well, but no agglomeration occurred. After short sonication, both dispersions were homogeneous (Fig. 2g), and preliminary results showed that their UV-Vis spectra indicated changes, such as disappearance of the absorption at 300 nm and increase in the absorption intensity, indicative of partial reduction of GO.

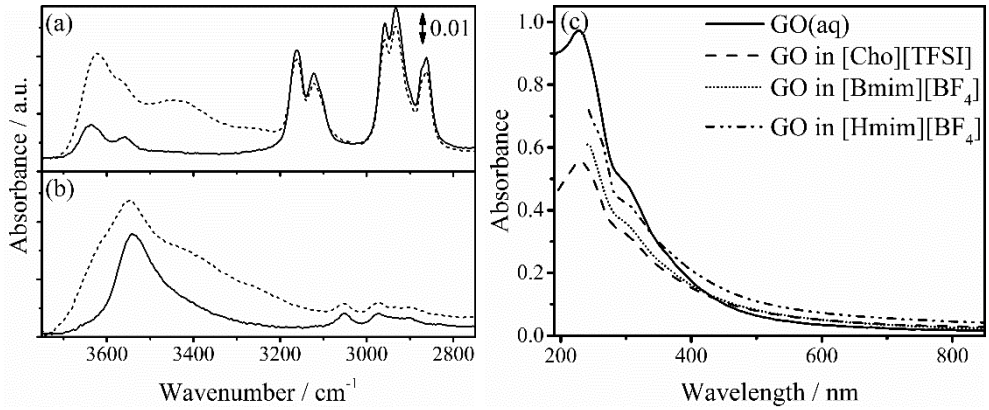

Figure 3. *(a-b) IR spectra of wet (dashed lines) and dried (solid lines) GO/IL dispersions: (a) 2 mg mL^{-1} GO in [Hmim][BF$_4$], and (b) 2 mg mL^{-1} GO in [Choline][TFSI]. (c) UV-Vis spectra of GO(aq) (solid line), 1.8 mg mL^{-1} GO in [Choline][TFSI] (dashed line), 2.0 mg mL^{-1} GO in [Bmim][BF$_4$] (dotted line) and 2.3 mg mL^{-1} GO in [Hmim][BF$_4$] (dash-dotted line).*

Solvothermal reduction of GO is one technique used for obtaining colloidal graphene suspensions [81,100].

6.2 Electrochemical polymerization and characterization of composites

In all electrochemical experiments, a coiled Pt wire and a Ag wire coated with AgCl served as counter and reference electrodes, respectively. The Ag/AgCl pseudo reference electrode was calibrated vs. ferrocene (Aldrich, 98 %) prior to use. The potential was controlled with either an Autolab PGSTAT101 (CV) or an IviumStat (electrochemical impedance spectroscopy (EIS)) potentiostat. A Pt-minielectrode (ø = 1 mm) was polished with diamond pastes (DP-Paste-P from Struers) of various grain sizes (0.25 – 3 µm) and carefully rinsed prior to serving as working electrode.

The monomers were added directly into the GO/IL dispersions with varying amounts of GO, and the electrochemical polymerization was performed by CV using a conventional one-compartment 3-electrode electrochemical setup. For comparison, polymer films were fabricated either using same amount of polymerization cycles or by accumulating same amount of charge. If we assume that the total charge consumed during electrochemical polymerization all goes into the formation of the polymer, the films should be similar in polymer content. The electrochemical polymerization of CPs can be done using galvanostatic, potentiostatic or potentiodynamic (CV) techniques. Most popular method of these three is the potentiostatic deposition. However, during potentiodynamic polymerization the process can be monitored better which is why CV was used to fabricate the films in this work. As it has been shown that GO can be effectively reduced by negative

potentials in various electrolytes [115,164], electrochemical reduction of GO was performed after the deposition of the composite films by cycling to -2.0 V over 30 cycles (Paper I) or to -1.9 V over 10 cycles (Paper II). Lower amount of cycles was used in Paper II due to the poor stability of PAz during cycling to negative potentials. Electroreduction of GO was also performed by drop-casting GO(aq) on a conducting substrate and cycling from 0.0 V to -2.0 V or -1.9 V in [Bmim][BF_4] and [Choline][TFSI], respectively. In both ILs, the reduction of GO was observed to begin around -0.4 V (vs. Ag/AgCl) with a broad peak around -1.0 V (vs. Ag/AgCl) in the first cycle. Since the reduction of GO appears to begin at quite high potentials, it is likely, that some reduction of GO already took place during electrochemical polymerization.

The as-produced films were characterized by CV and EIS before and after electroreduction, and in Papers II and V also after 1200 p-doping cycles. CV and EIS are the most common techniques used for evaluating the electrochemical doping behavior of CPs. EIS gives important information on the interfacial reactions. A typical Nyquist impedance plot of a CP can have a charge transfer resistance (R_{ct}) related semi-circle in the high frequency range followed by a Warburg diffusion line rising at 45° in the mid-frequencies, and ideally a vertical capacitive line is observed in the low frequency range. Capacitance can be determined from CV, the low frequency range of the Nyquist impedance plots or from galvanostatic charge/discharge experiments (GCD). GCD usually yields more accurate values, and it was therefore used in determining the capacitance of the devices in Paper V. Capacitances calculated by integrating the CVs give a good estimate whether a material can be considered a supercapacitor electrode or not. Therefore, CV was used for capacitance evaluation in 3-electrode configuration in Papers I, II and V. Firstly, the charge was obtained by integrating the forward scan of the CV, and from this the capacitance can be obtained by using a simple equation: $C = Q/U$, where C is the capacitance, Q is the charge that was passed during the forward scan and U is the voltage. Areal capacitance is further obtained by dividing the capacitance with the area of the electrode. In Paper V, another well-known strategy for obtaining the capacitance from CVs was additionally applied: CVs were recorded at several scan rates and the maximum currents plotted against the scan rates. The capacitance is obtained from the slope of the relation.

6.3 Spectroscopic and surface characterization of the films

In a typical study of composite materials, scanning electron microscopy (SEM), transmission electron microscopy (TEM), IR and Raman spectroscopies, X-ray photoelectron spectroscopy (XPS) and X-ray diffraction (XRD) are applied for determining the structural and chemical composition of the composites. In this work SEM, IR, Raman and XPS were applied. For spectroscopic and surface characterization, the films were fabricated on fluorine doped tin oxide (FTO) glass (K Glass from Pilkington with 8.1 Ω cm^2 sheet resistance) (IR, SEM, Raman) or on Au coated Si(111) wafers (Okmetic, Finland) (XPS). Polymer and composite films were polymerized on the glass or Si substrates, and carefully rinsed with organic solvents (dichloromethane) to remove any excess monomer-, oligomer- and IL-residues. However, despite exhaustive washing procedure, complete removal of IL from the films proved difficult which was observed by XPS analysis in Paper II, and has been reported also earlier [46].

Raman is an especially powerful tool for studying carbon based materials, and it is considered a complementary technique to IR. In both techniques, the molecule interacts with electromagnetic field, but for a molecule to be IR active, a change in dipole moment should take place whereas for a molecule to be Raman active, a change in polarization should occur. GO and rGO contain oxygen functionalities, and both IR spectroscopy and Raman spectroscopy can be applied to study their structure, especially to determine effective oxidation/reduction of the material [164,165]. Bruker Vertex 70 equipped with MCT detector and Harrick Seagull™ variable angle reflection accessory was applied for IR measurements, and Raman experiments were performed by Renishaw Ramascope (system 1000B) (Paper I) or Renishaw inVia QONTOR Raman microscope (Paper II) equipped with a Leica microscope and a charge-coupled device (CCD) detector. The scattering signal was collected at 180°.

6.4 *in situ* spectroelectrochemical characterization

The cell configurations used for *in situ* UV-Vis and attenuated total reflection (ATR) FTIR spectroelectrochemical analysis are presented in the supplementary information of Paper III, and detailed measurement conditions are given in Papers III and IV.

In the internal reflection mode of ATR-FTIR spectroscopy, the IR radiation approaches the electrode/electrolyte interphase from the optically denser material at an angle higher than the critical angle which results in total reflection of the beam (Fig. 4). At the point of incidence, a standing wave of the superimposed incoming and reflected IR beams is formed perpendicular to the surface, and when there is an absorbing substance placed on the reflecting element, the wave will interact with it resulting in the attenuation of the reflected beam. During *in situ* ATR-FTIR spectroelectrochemistry, the reflecting element is applied as the working electrode where the film under study is polymerized, and spectra are recorded during positive and/or negative doping of the film and compared to a reference spectrum. [149] We used a ZnSe hemisphere crystal (CRYSTRAN) as the reflecting element with a conducting layer of Pt in a Kretschmann type configuration with 68° angle of incidence. Spectra were recorded during polymerization and p-doping.

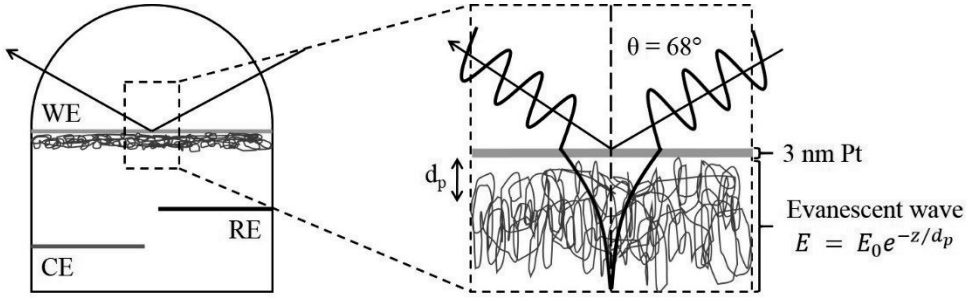

Figure 4. *Schematic representation of ATR-FTIR spectroscopy.*

7. SUMMARY OF RESULTS AND DISCUSSION

7.1 Composite fabrication

Composites of GO and ErGO with PEDOT were formed in two ionic liquids sharing the same small inorganic anion ($[BF_4]^-$) and an imidazolium-based cation with varying length of hydrocarbon substituents: a butyl group ($[Bmim]^+$) and a hexyl group ($[Hmim]^+$). This small change in the cation affects the water miscibility and the viscosity of the ILs already quite dramatically [166]. For comparison, PEDOT/PSS and PEDOT/GO composite films were also fabricated in water. PAz/GO composite films were formed in [Choline][TFSI] and in $[Hmim][BF_4]$, but in the latter IL the performance of the films was found to be poor.

Using potentiodynamic technique for polymerization enables the comparison between the formation of composite and polymer films. In general, the composite film formation was found to be similar to the polymer film formation as can be seen from the CVs shown in Fig. 5 for PAz based materials. All composite films showed increasing current of characteristic polymer redox responses as the polymerization proceeded indicating growth of an electroactive film. The composite films had good adhesion on all the applied substrates.

In Paper IV, polymerization of PEDOT/GO film in aqueous electrolyte was found to be much slower than PEDOT/PSS film formation, which corroborated previous studies conducted with potentiostatic polymerizations where the low pH of the GO(aq) solution resulted in the carboxyl groups to be in their protonated state thus hindering EDOT polymerization [121]. In water, GO carries a negative charge, which has been shown by zeta potential measurements [130], and it is entrapped in the film as the solemn counter anion. In IL, GO interacts with the cations of the IL through at least π-π interactions or van der Waals forces, and the main counter anion is most likely the IL anions, in this case either $[BF_4]^-$ or $[TFSI]^-$. How GO is incorporated, when the composite is formed in IL, is purely speculative and, although it has been suggested that it would act as counter anion, a more likely route is mechanical entrapment. The deposition rate of the composite films in ILs was found slightly faster compared to polymer film formation in Papers I and IV. In Paper I the accelerated film formation was attributed to the charged GO which is adsorbed to the electrode along with the IL. The presence of large counter anions has been shown to be beneficial for EDOT polymerization, but the faster film formation can also be caused by water impurities; even small amounts of water affects the physicochemical properties of imidazolium ILs [166], and the analysis showed that small amount of water remains in the suspensions.

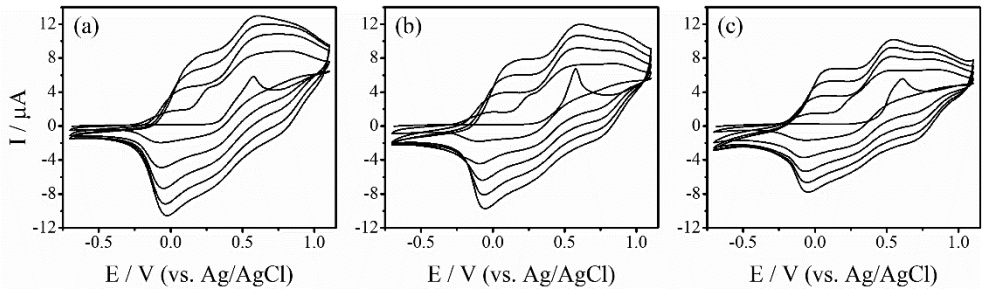

Figure 5. *Multicycle voltammograms of the first 5 polymerization cycles of (a) azulene, (b) azulene and 1 mg mL^{-1} GO, and (c) azulene and 2 mg mL^{-1} GO. Azulene concentration was 0.05 M.*

The polymerizations in the ILs was performed in the presence of different concentrations of GO, since the properties of nanocomposites are dependent on the ratios between the different components. In the SEM images of [126], it can be clearly seen that increasing the amount of GO in the polymerization medium also increases the amount of GO in the composite film. For PEDOT composites, highest electroactivity was obtained using a GO-concentration of 2 mg mL^{-1} while 1 mg mL^{-1} GO concentration appeared to form the most electroactive PAz composites (Fig. 6). The optimum GO concentration is dependent on the formation of an effective three-dimensional structure [I] but it also has to depend on the synthesis route of GO since GO materials vary in terms of relative amount of functional groups according to the graphite starting material and the applied oxidation method. The storage time and method (dried or in aqueous solution) can also change the structure of GO which has been described a dynamic material [167].

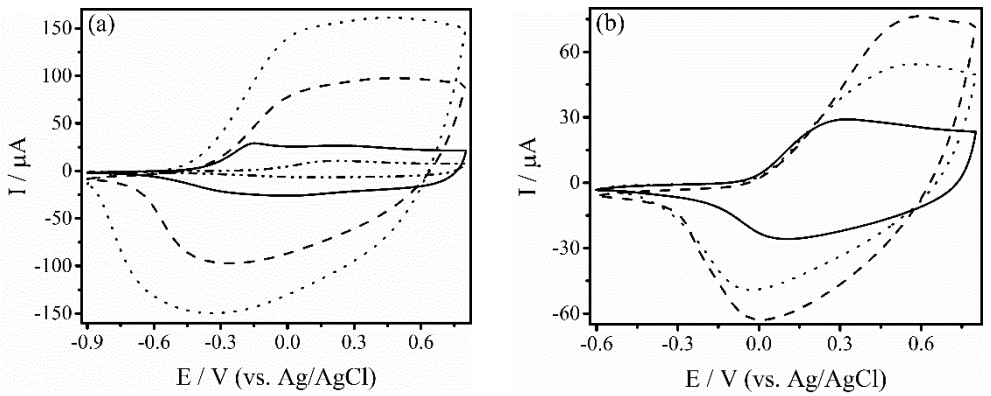

Figure 6. *Influence of GO concentration on the electroactivity of (a) PEDOT/GO [I] and (b) PAz/GO composite films [II]. Concentration of EDOT was 0.1 M, and azulene concentration was 0.05 M.*

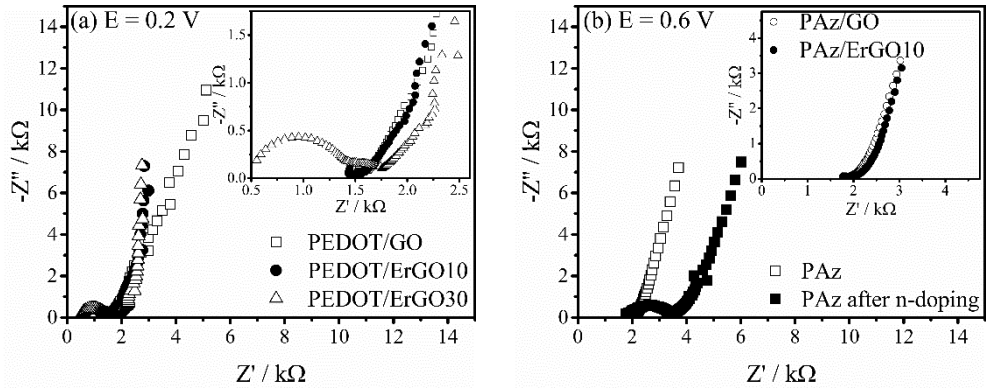

Figure 7. *Complex Nyquist impedance plots: (a) PEDOT/GO (□) and PEDOT/ErGO composites after 10 (●) and 30 (Δ) reduction cycles. Inset shows the low frequency range. [I] (b) PAz after polymerization (□) and after n-doping for 10 cycles (■). The inset shows the plots for PAz/GO (○) and PAz/ErGO (●) composites. [II]*

Another optimized parameter was the amount of electroreduction cycles. PEDOT/GO films were cycled between -0.4 and -2.0 V using 10, 20 and 30 cycles at 50 mV s^{-1} scan rate in [Bmim][BF_4] in Paper I. In the CVs, the electroactivity was observed to increase and the shape changed towards more rectangular promising improved characteristics. In the complex Nyquist impedance plots, the capacitive low frequency line approached the ideal 90° vertical line but simultaneously two R_{ct} related semi-circles in the high frequency range emerged suggesting changes in morphology or chain packing (Paper I).

For PAz/GO composites the reduction cycles were limited to 10 due to polymer restrictions. The reduction step of GO could have been avoided by using graphene directly exfoliated from graphite which can be achieved by electrochemical exfoliation in ILs, for example. Several projects on the electrochemical exfoliation of graphite in ILs and in solvent mixtures were going on in the laboratory during the time this thesis work was done, but the exfoliation of graphite in these works was not satisfactory for composite film formation. Reduction did not improve the electroactivity of PAz/GO composites, but a decrease in the electroactivity of neat PAz films was detected after n-doping whereas the composite films seemed to retain their electroactivity better. In the complex Nyquist impedance plots, an increase of the R_{ct} related semi-circle of PAz could be seen indicating polymer degradation (Fig. 7b).

7.2 Chemical and structural composition

The composition of the films was determined by SEM, XPS, IR, UV-Vis and Raman spectroscopies which are common techniques for the assessment of composite materials. IR spectroscopy and XPS appeared to be poor characterization

techniques for these composite films. In IR, the vibrations of the polymer, GO and rGO overlapped to a large extent, and the spectrum of the polymer governed the recorded IR spectra. The interpretation of XPS results, on the other hand, turned out quite tricky due to using ILs as electrolyte. ILs are difficult to completely remove from the film without removing the entire film from the substrate. Especially in Paper II, the presence of [Choline][TFSI] in the films could be verified by XPS from the C-F bonds in the C 1s spectra and F 1s spectra. Additionally, the hydroxyl group on cholinium was present in the C 1s spectra of PAz at 286.6 eV (C-O). This is usually attributed to the hydroxyl and epoxy groups of GO in these types of composites. The PAz/GO composite did, however, exhibit with higher relative amount of C-O and lower C:O ratio which was cautiously attributed to the incorporation and reduction of GO.

Raman spectroscopy revealed some key differences between the polymer and composite films. In the Raman spectra of PEDOT-based composites (λ_{exc} = 514 nm), small shoulders were observed at the characteristic G- (1590 cm^{-1}) and D-band (1300 cm^{-1}) Raman shifts of GO (Fig. 8a) while these bands were clearly visible in the Raman spectrum of PAz composites obtained using the excitation wavelength of 785 nm (Fig. 8b). PAz materials' spectra were also collected using another excitation wavelength (λ_{exc} = 532 nm), which lay closer to the π-π* transition of the polymer (430 nm). This excitation wavelength resonance enhanced the signals of the polymer film [155,168], and in these spectra only small shoulders of GO could be observed. Since the π-π* transition of PEDOT lies around 580 nm, measuring Raman with λ_{exc} = 514 nm has likely resonance enhanced the signals of the polymer which could explain why GO bands were only observed as weak shoulders in Paper I.

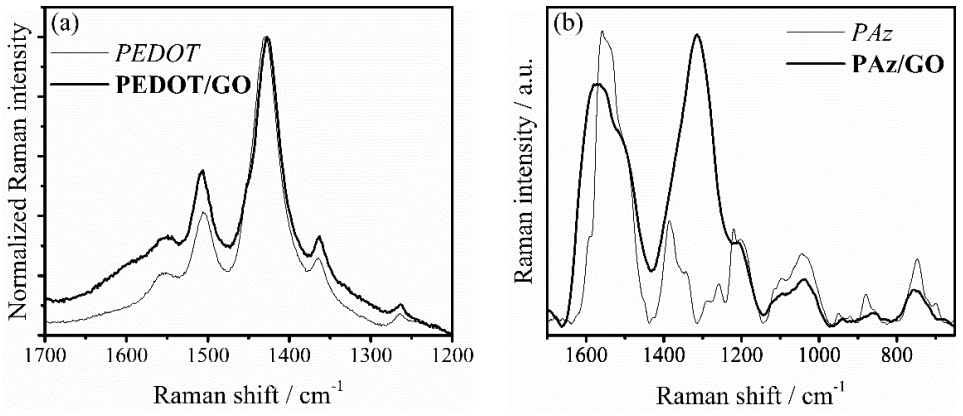

Figure 8. *Raman spectra of (a) PEDOT (thin line) and PEDOT/GO (thick line) measured with λ_{exc} = 514 nm [I], and (b) PAz (thin line) and PAz/GO (thick line) measured with λ_{exc} = 785 nm [II].*

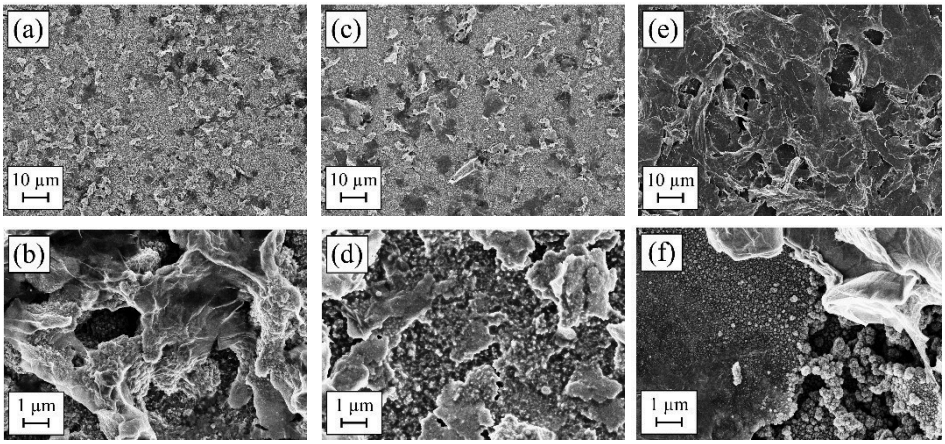

Figure 9. *SEM images of (a) PEDOT/GO and (b) PEDOT/ErGO made in [Bmim][BF_4], (c) PEDOT/GO and (d) PEDOT/ErGO made in [Hmim][BF_4] [I], and (e) PAz/GO and (f) PAz/ErGO [II]. The magnifications are 1000x (a, c and e) and 10000x (b, d and f).*

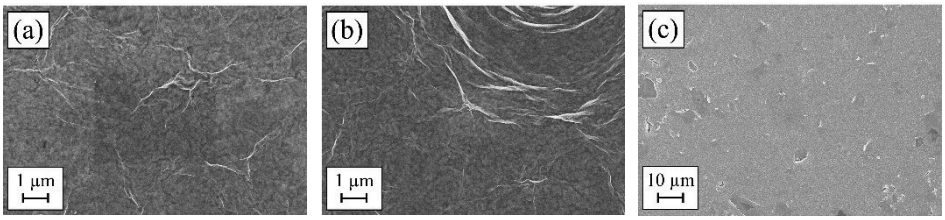

Figure 10. *SEM images of (a) PEDOT/GO and (b) and PEDOT/ErGO made in water. The magnification is 10000x. [I] (c) SEM image of PAz/ErGO made in [Hmim][BF_4] at 1000x magnification.*

The morphologies of the polymers were granule-like, and in the composites, crumpled sheets of GO and ErGO were uniformly distributed over the analyzed areas (Fig. 9). The morphology of the PEDOT-based composites was very similar before and after electroreduction independent of the IL but varied significantly from the composites formed in water (Fig. 10a-b) (Paper I). Interestingly, the microstructures of PAz-based composites were different before and after reduction: PAz/GO showed a GO-governed, compact film with some bigger holes (Fig. 9e) and PAz/ErGO composite showed porous polymer matrix with embedded sheets of ErGO (Fig. 9f) (Paper II), similar to PEDOT-based composites. PAz/GO composites were also fabricated in [Hmim][BF_4], but the electrochemical properties of these films were poor. Fig. 10c shows a SEM image of PAz/ErGO composite made in [Hmim][BF_4], and as can be seen the film structure is very compact with only few sheets of GO visible in the analyzed area. In Paper V we discovered that PAz morphology varies significantly depending on the polymerization IL, and in the lowest viscosity ILs the microstructure resembled those seen in organic solvents, but in [Hmim][BF_4] large, poorly connected granules were obtained. Previously reported composites of

PEDOT and GO fabricated in water electrochemically show similar compact morphology independent of electropolymerization technique [121,127,131]. Similarly, compact microstructures have been reported for PANi-based composites [124] and PPy-based composites [118,120]. Interestingly, composite of PEDOT and rGO polymerized from an aqueous dispersion of rGO showed a very porous microstructure [125], as did composite of GO and poly(N-methylaniline) [128]. It is well-established that polymerization of CPs in ILs produces films with very different morphologies from their counterparts made in conventional solvents, which explains the porous polymer structure seen in our films. The microstructure of the composite films likely depends on whether GO is used as the main dopant or as co-dopant, and also on the procedures preceding the polymerization, for example ultrasonication times (long periods of sonication can break GO down to smaller flakes).

7.3 Electrochemical properties

When cycled at faster scan rates (>20 mV s^{-1}), the CVs of PAz-based composite films showed increased difference between the peak oxidation (E_{pa}) and reduction potentials (E_{pc}) compared to PAz (Fig. 6b). We speculated in Paper II that this could originate from (i) the resistive behavior of GO in the composite film, (ii) the formation of thicker films, or (iii) the compact microstructure which could have hindered ion diffusion. On the other hand, later studies by *in situ* spectroelectrochemistry in Paper III suggested that PAz might form shorter conjugation length during polymerization in the presence of GO which can make the material less conducting and cause an increase of ΔE. When characterized with very slow scan rates (2 mV s^{-1}), three oxidation and two reduction responses for the composite film appeared while two redox couples were observed for the polymer film in IL (Fig. 11a). Upon cycling the films in acetonitrile (Fig. 11b), the composite film oxidation and reduction responses were at substantially higher potentials compared to the polymer film, corroborating the finding of shorter conjugation in Paper III.

In the slow scan rate CVs of PAz in Paper III, indications of charge trapping in the form of pre-peaks could also be distinguished. Upon cycling PEDOT and PEDOT/GO films made in IL using water (Fig. 11c) and organic electrolytes, PEDOT film had a very sharp pre-peak while in the composite CVs this pre-peak was much broader or even absent in acetonitrile. Both PEDOT/PSS and PEDOT/GO films formed in water showed sharp pre-peaks of similar shape and magnitude in all the studied electrolytes. The films made in water also showed R_{ct} related semi-circles in the complex impedance plots upon applying IL or acetonitrile electrolyte, while PEDOT/GO composite formed in [Bmim][BF_4] exhibited capacitive lines

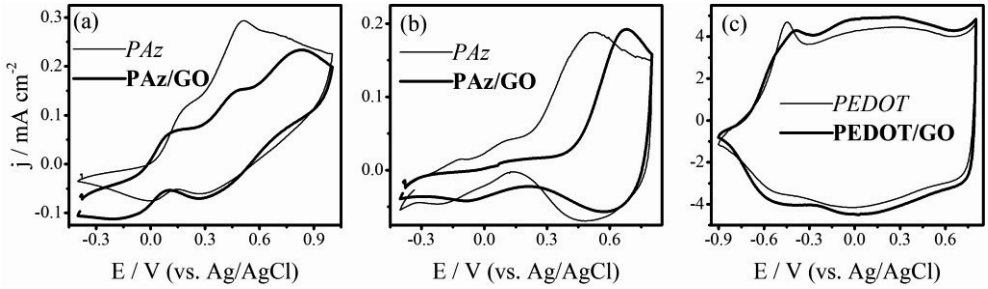

Figure 11. *(a-b) CVs of p-doping PAz (thin line) and PAz/GO (thick line) at 2 mV s^{-1} in (a) [Choline][TFSI] and (b) 0.1 M TBA-BF_4 in ACN on ZnSe crystal. [III] (c) CVs of p-doping PEDOT (thin line) and PEDOT/GO (thick line) at 100 mV s^{-1} in 0.1 M KCl(aq) on Pt-minielectrode. [IV]*

throughout the frequency range. This proves the enhanced charge transport in the IL-based composite compared to materials made in water.

Capacitance in 3-electrode setup was evaluated from CVs. The CVs of PAz/GO composites showed deviation from the ideally rectangular shape at higher scan rates ($\leq$50 mV s^{-1}), and their capacitance decreased to slightly less than half of the initial value as the scan rate increased from 20 to 200 mV s^{-1} (Fig. 12a). [Choline][TFSI] with a reported viscosity of 93.4 cP at 30 °C [169] was partially blamed for this behavior since high viscosity results in slow mass transport, but GO and short conjugation could affect as well. The capacitance of PEDOT-based films is substantially lower than the capacitance of PAz-based materials, but PEDOT-based films are less dependent on the scan rate since at 500 mV s^{-1} they still have retained over 85 % of their initial capacitance (Fig. 12b). Better rate capability of PEDOT-based films is explained by the better conductivity of PEDOT (highest reported conductivity of PAz is 2.2 S cm^{-1} [145] and the conductivity of electropolymerized PEDOT is 10 S cm^{-1} [170]). PEDOT-based films polymerized in IL show higher capacitance values than PEDOT/PSS and PEDOT/GO films fabricated in water. The PEDOT/GO made in water showed higher capacitance than PEDOT/PSS throughout the scan rate range studied, but the films made in IL behaved differently. Surprisingly, the capacitance of the composite film made in IL was similar or even lower than the polymer film capacitance at low scan rates (< 100 mV s^{-1}) and only at faster scan rates, the capacitance of the composite film was substantially higher than the polymer film capacitance indicating that the composite film made in IL had better rate-capability over the polymer film.

One of the main drives for fabricating composites is to improve the cycling stability of pseudocapacitors. To be an eligible candidate for SCs, the electrode material should exhibit almost negligible capacitance loss over several thousand cycles, and a loss of 30 % is considered end-of-life for the devices [136].

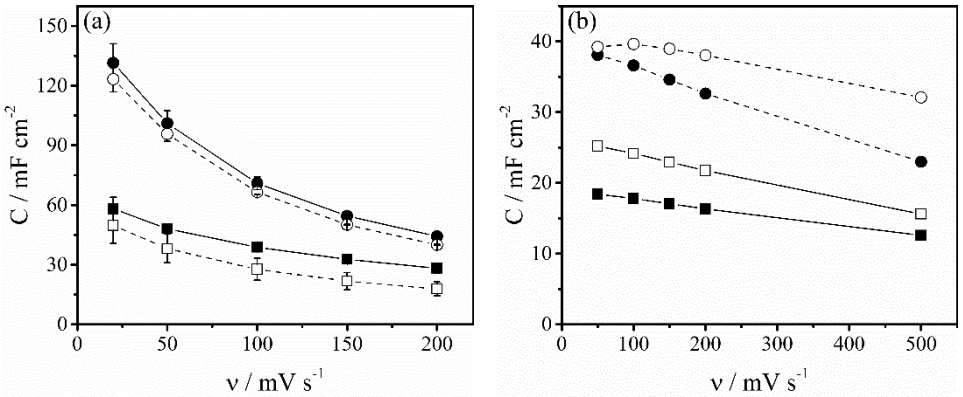

Figure 12. *(a) Areal capacitance of PAz (■) and PAz/GO fabricated using 1 mg mL^{-1} GO (●) after polymerization (solid symbols) and long-term cycling (empty symbols). [II] (b) Areal capacitances of PEDOT/PSS (■), PEDOT/GO(aq) (□), PEDOT(IL) (●) and PEDOT/GO(IL) (○) in [Bmim][BF$_4$]. The capacitances were evaluated from CVs.*

In this study, the materials were studied by cycling them for 800 (Paper I) or 1200 (Papers II and V) cycles. All films retained over 85 % of their capacitance during the cycling test showing slight tendency that the composite films retain their properties better. However, in the experimental conditions of this work, the differences between the polymer films and the composite films in terms of long term cycling stability were very small. As PEDOT already in itself is quite stable a polymer, the long-term cycling performance perhaps does not improve to such a large extent for PEDOT based nanocomposites. Electropolymerized PEDOT/PSS, PEDOT/GO and PEDOT/rGO exhibited capacitance losses of 10.7 %, 9.9 % and 13.9 %, respectively, in 3-electrode configuration over 3000 cycles [143]. On other occasions, increase of capacitance has been demonstrated in a 3-electrode cell during 10000 cycles but a decrease occurs in a device configuration [124]. Cycling stability also depends on the applied potential range [143]. Minor improvement of the cycling stability may also just be a property of the electrochemically fabricated composites as it would appear that chemically prepared nanocomposites sometimes show significant improvements in long-term cycling performance, as can be seen from the values gathered in Table 1 (Chapter 3.3). PAz did, however, show improved cycling stability in ILs compared to organic solvents (Paper V) which is a common feature observed for CPs. The EIS analysis was repeated after long-term cycling, and for PAz the R_{ct} related semi-circle observed in the high frequency range grew substantially while impedance plots of the composite film showed much smaller changes indicating improved long-term cycling stability for the composite film.

7.3.1 Performance in bendable devices

Capacitance of PAz had been previously determined in organic solvents in 3-electrode configuration [146], and the result suggested that PAz could have similar capacitive properties to PANi which holds the highest capacitance values of CPs [134]. However, the performance can be very different in a device configuration, and also the electroactivity of PAz had been shown to improve upon using ILs [32]. Therefore, in Paper V we studied the capacitance of PAz in three different ILs with varying cations, anions and viscosities in a 3-electrode configuration by CV and EIS as well as determined the performance of PAz in symmetric and asymmetric supercapacitor configurations. Naturally, the capacitance of PAz measured in 3-electrode cell was highest in the lowest viscosity IL and lowest in the highest viscosity IL since viscosity affects the mass transport (Fig. 13a). Also, in [Emim][TFSI] the rate capability was found much better than in the two higher viscosity ILs.

By using electrochemical fabrication, we could directly apply the films on bendable substrates, and both symmetric and asymmetric devices were characterized. In device configuration, only [Choline][TFSI] served as electrolyte and, although PAz was polymerized also in [Emim][TFSI], the device performances were very similar. PAz turned out to perform very poorly in a symmetric configuration due to undoping of the negative electrode which is why it was replaced with AC for asymmetric devices. The asymmetric devices had a capacitance of 27 mF cm^{-2} and equivalent series resistance (ESR) of 19 Ω at 1.5 V cell voltage (Paper V). Using IL as electrolyte allowed us to increase the cell voltage up to 2.4 V, and the capacitance and energy increased by 33 % and 240 %, respectively, (Fig. 13b). The maximum voltage of 2.4 V is low compared to some of the records obtained using ILs as electrolytes in SCs and it is similar or lower to organic electrolytes, but ILs are considered safer than organic solvents due to their negligible vapor pressure. The devices were also bent down to a radius of 1.5 cm, which did not affect the capacitance (Fig. 13c).

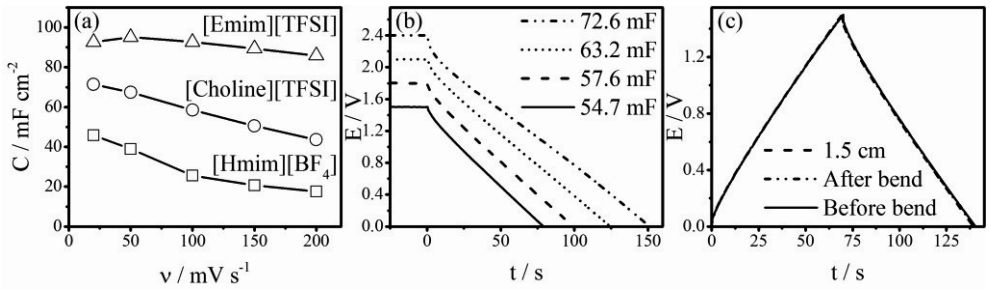

Figure 13. *(a) Areal capacitance of PAz films in different ILs using 3-electrode configuration. (b) Discharge and (c) charge/discharge curves of asymmetric PAz supercapacitors. [V]*

7.4 Electronic properties and charge carrier formation

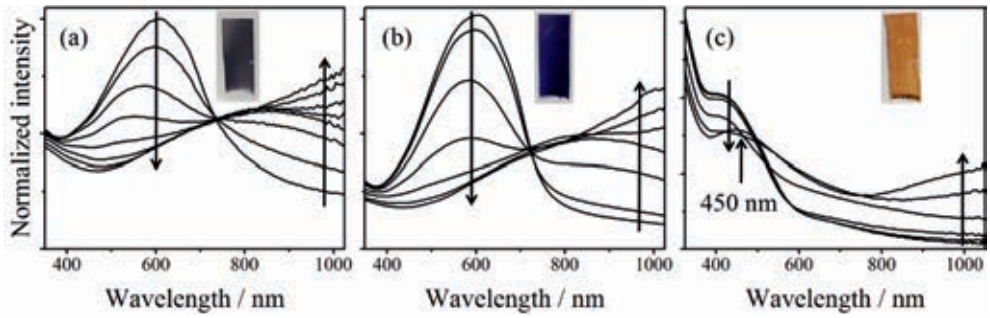

Figure 14. *The UV-Vis spectra of composite films obtained in situ during anodic scan of p-doping. (a) PEDOT/GO(aq) from -0.7 to 0.7 V. (b) PEDOT/GO(IL) from -0.4 to 0.8 V. [IV] (c) PAz/GO from 0.0 to 1.0 V. [III]*

In the UV-Vis spectra recorded *in situ* during p-doping, all films showed bleaching of the neutral polymers π-π* transition related absorption band accompanied by the growth of new bands related to the formation of the charge carriers: PEDOT-based films above 800 nm, and PAz-based films above 800 nm and at 450 nm (Fig. 14) (Papers III and IV). At the end of the p-doping cycle, the initial state was reinstated for all the studied films showing that the materials had good reversibility, and the composite films fabricated in ILs had their absorption bands at similar wavelengths as the polymer films, and the changes in the spectra took place at similar potentials. The only films showing more differences compared to each other were the PEDOT/PSS and PEDOT/GO films fabricated in aqueous solution (Fig. 14a). The π-π* transition related absorption band of the composite film laid at higher wavelength, and the appearance of the film was gauzy compared to the light blue color of PEDOT/PSS.

Composite film fabrication was followed by *in situ* ATR-FTIR spectroelectrochemistry during the first five polymerization cycles and compared to the growth to the corresponding polymer film's spectra. In the high wavenumber region, one broad electronic absorption was observed for PEDOT/GO film in IL, and it showed a decreasing tendency after the 2nd polymerization cycle while PEDOT film's electronic absorption became more intense during the experiment (Paper IV). This shows that incorporating GO into PEDOT causes some changes in the packing of the film. For both PAz and PAz/GO film, two differently behaving absorptions were observed during polymerization in IL while single broad electronic absorption grew in the spectra of PAz polymerized in acetonitrile (Paper III). We speculated that this could be an indication of two differently behaving charge carriers in PAz as this type of behavior had been previously pointed out in the literature [14,155,157].

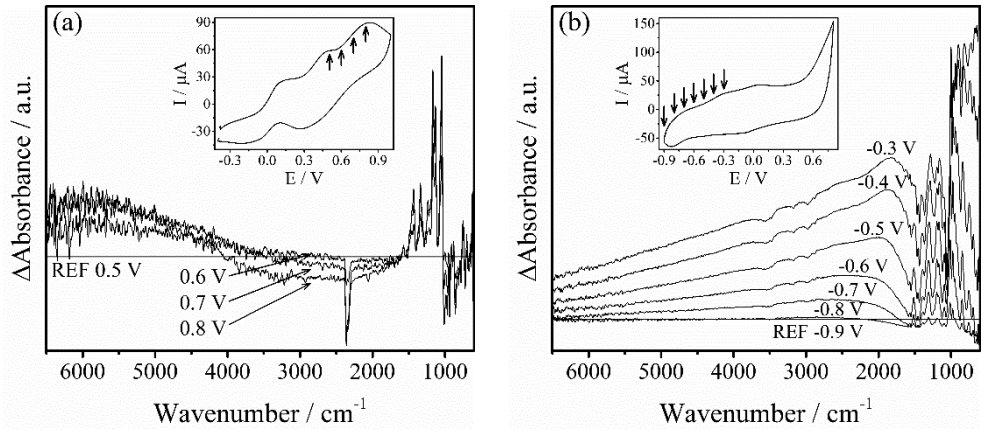

Figure 15. *The in situ ATR-FTIR spectra in the range from 6500 cm^{-1} to 700 cm^{-1} obtained during the anodic scan of p-doping for (a) PAz/GO composite in [Choline][TFSI] [III] and (b) PEDOT/GO(IL) composite in [Bmim][BF_4] [IV]. The potentials are indicated in the figures, and the insets show the corresponding CVs recorded at 2 mV s^{-1} scan rate.*

Spectra recorded during p-doping PAz and PAz/GO films also exhibited growth of broad electronic absorptions at higher wavenumbers. When a reference spectrum was chosen at a higher potential where the materials were already partially charged, two independently behaving absorption bands was revealed, a broad decreasing band around 3000 cm^{-1} and an increasing band around 5500 cm^{-1} (Fig. 15a) indicative of increase of polaron pairs and decrease in polarons (Paper III). During p-doping, PEDOT materials had only a single broad electronic absorption growing in the higher wavenumbers (Fig. 15b).

Growth of the electronic absorptions was accompanied by the appearance of new doping induced infrared active vibration (IRAV) bands in the lower wavenumber area which corresponded to the IRAV fingerprint of the polymers spectra for all materials (Fig. 16). Unfortunately, the interpretation of the IRAV bands of PAz-based films turned out to be difficult in [Choline][TFSI] since the strongest absorbance bands of the [TFSI] anion critically overlapped most of the IRAV bands of PAz, but in acetonitrile all PAz IRAV bands became visible: the IRAV bands of PAz were located at 1589, 1473, 1427, 1344, 1190, 1053, 879 and 752 cm^{-1}, while the IRAV bands of the composite were found at slightly higher wavenumbers at 1595, 1487, 1421, 1350, 1203, 1056, 894 and 754 cm^{-1} (Paper III). The small shift towards higher wavenumbers was interpreted as shortening in the effective conjugation length of the polymer in the presence of GO. In the spectra of PEDOT-based films, the vibration bands of the IL were observed as an increasingly negative band, contrary to what was observed in Paper III for [Choline][TFSI], and the IRAV bands of PEDOT and the composite were located at similar wavelengths indicating that incorporation of GO does not affect PEDOT conjugation.

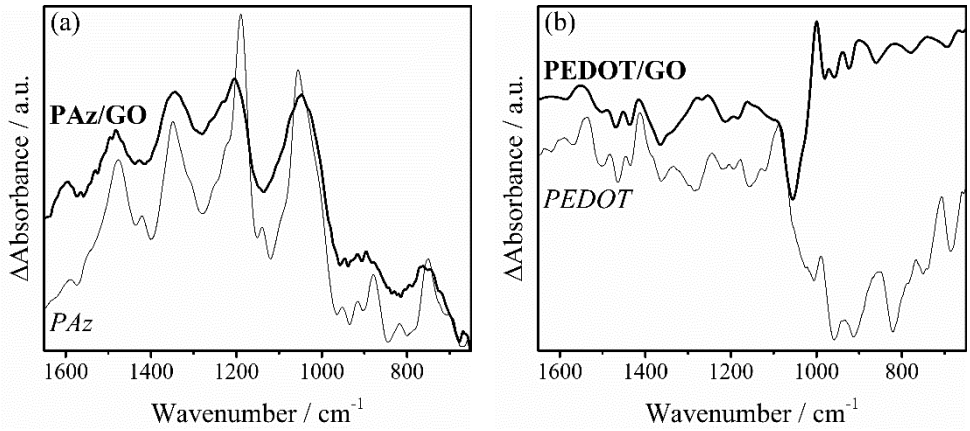

Figure 16. *The in situ ATR-FTIR spectra in the range from 1650 cm^{-1} to 650 cm^{-1} of (a) PAz (thin line) and PAz/GO composite (thick line) in 0.1 M TBA-BF_4 in ACN at 0.6 V [III], and (b) PEDOT (thin line) and PEDOT/GO composite (thick line) in [Bmim][BF_4] at 0.1 V [IV]. For PAz films the reference spectrum was obtained at 0.0 V, for PEDOT at -0.7 V and for PEDOT/GO film at -0.9 V.*

8. CONCLUSIONS AND FUTURE OUTLOOK

Although promising materials, conducting polymer-graphene nanocomposites have a long road ahead to be used in actual devices, and have especially recently received some criticism, since despite huge effort, the long-term cycling stability remains too low. In a supercapacitor device, all the pieces in the puzzle (electrode material, electrolyte, current collectors) affect the final picture, and therefore no material should be overlooked.

The work conducted in this project is a very basic study on some conducting polymer-reduced graphene oxide nanocomposites. It shows, that nanocomposites between conducting polymers and electrochemically reduced graphene oxide can be produced from stable suspension of GO in ionic liquids with a facile electrochemical approach. The electrochemical approach, although produces materials with lower energy content than chemically made films, does not burden the environment to similar extent, and if biomolecule based ionic liquids would be utilized, the eco-friendliness of this process could be further improved. By using electrochemistry, one-pot synthesis of CP/rGO composite electrodes is possible if suitable potential ranges are applied during electrochemical polymerization, and the approach can be scaled-up to make small bendable devices, although the energy densities obtained herewith are low compared to some record-high values reported in literature. Using GO as a dopant during the polymerization is an efficient way to incorporate it inside the polymer matrix, but it needs to be reduced back to its conducting form. Since some polymers, PAz included, are sensitive to very negative potentials, an approach where exfoliated graphite is used as graphene-precursor might be a better option. The electrochemical characteristics of the materials made in this work have been studied in 3-electrode setups and in device configurations, and their composition has been thoroughly characterized. As ionic liquids already have the ability to improve conducting polymer film electroactivity and long-term cycling stability, the addition of large ErGO sheets only slightly improved these properties further. In this work, the possibility of using a "new" conducting polymer, polyazulene, as a supercapacitor electrode material has been further studied. The first bendable symmetric and asymmetric PAz supercapacitors were fabricated and characterized in this work, and their capacitive properties were good.

This work also presents an effort to understand the interactions between the conducting polymer and GO in the nanocomposites better, and how the incorporation of GO might affect the polymers electronic and charge carrier behavior. While PEDOT has yet again proven to be a robust polymer that does not change from additional dopants, PAz appears to be more susceptible to changes in the polymerization environment.

REFERENCES

[1] A. Burke, Ultracapacitor technologies and application in hybrid and electric vehicles, Int. J. Energy Res. 34 (2010) 133–151.

[2] A.M. Österholm, D.E. Shen, A.L. Dyer, J.R. Reynolds, Optimization of PEDOT films in ionic liquid supercapacitors: demonstration as a power source for polymer electrochromic devices, ACS Appl. Mater. Interfaces. 5 (2013) 13432–13440.

[3] B.E. Conway, Electrochemical Supercapacitors: Scientific Fundamentals and technological Applications, Springer US, New York, 1999.

[4] E. Frackowiak, F. Béguin, Electrochemical storage of energy in carbon nanotubes and nanostructured carbons, Carbon 40 (2002) 1775–1787.

[5] M.D. Stoller, S. Park, Y. Zhu, J. An, R.S. Ruoff, Graphene-Based Ultracapacitors, Nano Lett. 8 (2008) 3498–3502.

[6] B.E. Conway, V. Birss, J. Wojtowicz, The role and utilization of pseudocapacitance for energy storage by supercapacitors, J. Power Sources. 66 (1997) 1–14.

[7] D.P. Dubal, O. Ayyad, V. Ruiz, P. Gómez-Romero, Hybrid energy storage: the merging of battery and supercapacitor chemistries, Chem. Soc. Rev. 44 (2015) 1777–1790.

[8] J.D. Stenger-Smith, C.K. Webber, N. Anderson, A.P. Chafin, K. Zong, J.R. Reynolds, Poly(3,4-alkylenedioxythiophene)-Based Supercapacitors Using Ionic Liquids as Supporting Electrolytes, J. Electrochem. Soc. 149 (2002) A973–A977.

[9] W. Lu, A.G. Fadeev, B. Qi, E. Smela, B.R. Mattes, J. Ding, G.M. Spinks, J. Mazurkiewicz, D. Zhou, G.G. Wallace, D.R. MacFarlane, S.A. Forsyth, M. Forsyth, Use of Ionic Liquids for pi -Conjugated Polymer Electrochemical Devices, Science 297 (2002) 983–987.

[10] J. Ding, D. Zhou, G. Spinks, G. Wallace, S. Forsyth, M. Forsyth, D. MacFarlane, Use of ionic liquids as electrolytes in electromechanical actuator systems based on inherently conducting polymers, Chem. Mater. 15 (2003) 2392–2398.

[11] M. Kalbáč, L. Kavan, M. Zukalová, L. Dunsch, An in situ Raman spectroelectrochemical study of the controlled doping of single walled carbon nanotubes in a conducting polymer matrix, Carbon 45 (2007) 1463–1470.

[12] M. Kalbáč, L. Kavan, L. Dunsch, An in situ Raman spectroelectrochemical study of the controlled doping of semiconducting single walled carbon nanotubes in a conducting polymer matrix, Synth. Met. 159 (2009) 2245–2248.

[13] P. Damlin, C. Kvarnström, A. Nybäck, M. Käldström, A. Ivaska, Electrochemical and spectroelectrochemical study on bilayer films composed of C60 and poly(3,4-ethylenedioxythiophene) PEDOT, Electrochim. Acta. 51 (2006) 6060–6068.

[14] A. Österholm, P. Damlin, C. Kvarnström, A. Ivaska, Studying electronic transport in polyazulene-ionic liquid systems using infrared vibrational spectroscopy., Phys. Chem. Chem. Phys. 13 (2011) 11254–11263.

[15] H. Ohno, ed., Electrochemical Aspects of Ionic Liquids, 1st ed., John Wiley & Sons, New Jersey, 2005.

[16] J.S. Wilkes, M.J. Zaworotko, Air and Water Stable 1-Ethyl-3-methylimidazolium Based Ionic Liquids, J. Chem. Soc. Chem. Commun. (1992) 965–967.

[17] P. Hapiot, C. Lagrost, Electrochemical reactivity in room-temperature ionic liquids, Chem. Rev. 108 (2008) 2238–2264.

[18] J.G. Huddleston, A.E. Visser, W.M. Reichert, H.D. Willauer, G.A. Broker, R.D. Rogers, Characterization and comparison of hydrophilic and hydrophobic room temperature ionic liquids incorporating the imidazolium cation, Green Chem. 3 (2001) 156–164.

[19] R.P. Swatloski, J.D. Holbrey, R.D. Rogers, Ionic liquids are not always green: hydrolysis of 1-butyl-3-methylimidazolium hexafluorophosphate, Green Chem. 5 (2003) 361–363.

[20] N. Gathergood, M.T. Garcia, P.J. Scammells, Biodegradable ionic liquids: Part I. Concept, preliminary targets and evaluation, Green Chem. 6 (2004) 166–175.

[21] M.T. Garcia, N. Gathergood, P.J. Scammells, Biodegradable ionic liquids : Part II. Effect of the anion and toxicology, Green Chem. 7 (2005) 9–14.

[22] N. Gathergood, P.J. Scammells, M.T. Garcia, Biodegradable ionic liquids : Part III. The first readily biodegradable ionic liquids, Green Chem. 8 (2006) 156–160.

[23] K. Fukumoto, M. Yoshizawa, H. Ohno, Room Temperature Ionic Liquids from 20 Natural Amino Acids, J. Am. Chem. Soc. 127 (2005) 2398–2399.

[24] Y. Fukaya, Y. Iizuka, K. Sekikawa, H. Ohno, Bio ionic liquids: room temperature ionic liquids composed wholly of biomaterials, Green Chem. 9 (2007) 1155–1157.

[25] Q.-P. Liu, X.-D. Hou, N. Li, M.-H. Zong, Ionic liquids from renewable biomaterials: synthesis, characterization and application in the pretreatment of biomass, Green Chem. 14 (2012) 304–307.

[26] J.-Y. Kim, J.-T. Kim, E.-A. Song, Y.-K. Min, H. Hamaguchi, Polypyrrole Nanostructures Self-Assembled in Magnetic Ionic Liquid as a Template, Macromolecules. 41 (2008) 2886–2889.

[27] Y. Pang, H. Xu, X. Li, H. Ding, Y. Cheng, G. Shi, L. Jin, Electrochemical synthesis, characterization, and electrochromic properties of poly(3-chlorothiophene) and its copolymer with 3-methylthiophene in a room temperature ionic liquid, Electrochem. Commun. 8 (2006) 1757–1763.

[28] P.S. Murray, S.F. Ralph, C.O. Too, G.G. Wallace, Electrosynthesis of novel photochemically active inherently conducting polymers using an ionic liquid electrolyte, Electrochim. Acta. 51 (2006) 2471–2476.

[29] H. Shirakawa, E.J. Louis, A.G. MacDiarmid, C.K. Chiang, A.J. Heeger, Synthesis of Electrically Conducting Organic Polymers : Halogen Derivatives of Polyacetylene, (CH)x, J. Chem. Soc. Chem. Comm. (1977) 578–580.

[30] T.A. Skotheim, J.R. Reynolds, eds., Handbook of Conducting Polymers: Conjugated Polymers - Theory, Synthesis, Properties, and Characterization, 3rd ed., CRC Press, Taylor & Francis Group, New York, 2007.

[31] C. Lagrost, D. Carrié, M. Vaultier, P. Hapiot, Reactivities of Some Electrogenerated Organic Cation Radicals in Room-Temperature Ionic Liquids: Toward an Alternative to Volatile Organic Solvents?, J. Phys. Chem. A. 107 (2003) 745–752.

[32] A. Österholm, C. Kvarnström, A. Ivaska, Ionic liquids in electrosynthesis and characterization of a polyazulene-fullerene composite, Electrochim. Acta. 56 (2011) 1490–1497.

[33] K. Sekiguchi, M. Atobe, T. Fuchigami, Electropolymerization of pyrrole in 1-ethyl-3-methylimidazolium trifluoromethanesulfonate room temperature ionic liquid, Electrochem. Commun. 4 (2002) 881–885.

[34] K. Sekiguchi, M. Atobe, T. Fuchigami, Electrooxidative polymerization of aromatic compounds in 1-ethyl-3-methylimidazolium trifluoromethanesulfonate room-temperature ionic liquid, J. Electroanal. Chem. 557 (2003) 1–7.

[35] J.M. Pringle, J. Efthimiadis, P.C. Howlett, J. Efthimiadis, D.R. MacFarlane, A.B. Chaplin, S.B. Hall, D.L. Officer, G.G. Wallace, M. Forsyth, Electrochemical synthesis of polypyrrole in ionic liquids, Polymer 45 (2004) 1447–1453.

[36] K. Wagner, J.M. Pringle, S.B. Hall, M. Forsyth, D.R. MacFarlane, D.L. Officer, Investigation of the electropolymerisation of EDOT in ionic liquids, Synth. Met. 153 (2005) 257–260.

[37] J.M. Pringle, M. Forsyth, D.R. MacFarlane, K. Wagner, S.B. Hall, D.L. Officer, The influence of the monomer and the ionic liquid on the electrochemical preparation of polythiophene, Polymer 46 (2005) 2047–2058.

[38] M. Biso, M. Mastragostino, M. Montanino, S. Passerini, F. Soavi, Electropolymerization of poly(3-methylthiophene) in pyrrolidinium-based ionic liquids for hybrid supercapacitors, Electrochim. Acta. 53 (2008) 7967–7971.

[39] P.C. Innis, J. Mazurkiewicz, T. Nguyen, G.G. Wallace, D. MacFarlane, Enhanced electrochemical stability of polyaniline in ionic liquids, Curr. Appl. Phys. 4 (2004) 389–393.

[40] K. Liu, Z. Hu, R. Xue, J. Zhang, J. Zhu, Electropolymerization of high stable poly(3,4-ethylenedioxythiophene) in ionic liquids and its potential applications in electrochemical capacitor, J. Power Sources. 179 (2008) 858–862.

[41] J.H. Mazurkiewicz, P.C. Innis, G.G. Wallace, D.R. MacFarlane, M. Forsyth, Conducting Polymer Electrochemistry in Ionic Liquids., Synth. Met. 135–136 (2003) 31–32.

[42] W. Lu, A.G. Fadeev, B. Qi, B.R. Mattes, Stable Conducting Polymer Electrochemical Devices Incorporating Ionic Liquids, Synth. Met. 135–136 (2003) 139–140.

[43] A. Balducci, W.A. Henderson, M. Mastragostino, S. Passerini, P. Simon, F. Soavi, Cycling stability of a hybrid activated carbon//poly(3-methylthiophene) supercapacitor with N-butyl-N-methylpyrrolidinium bis(trifluoromethanesulfonyl)imide ionic liquid as electrolyte, Electrochim. Acta. 50 (2005) 2233–2237.

[44] P. Damlin, C. Kvarnström, A. Ivaska, Electrochemical synthesis and in situ spectroelectrochemical characterization of poly(3,4-ethylenedioxythiophene) (PEDOT) in room temperature ionic liquids, J. Electroanal. Chem. 570 (2004) 113–122.

[45] F.F.C. Bazito, L.T. Silveira, R.M. Torresi, S.I. Córdoba de Torresi, On the stabilization of conducting pernigraniline salt by the synthesis and oxidation of polyaniline in hydrophobic ionic liquids, Phys. Chem. Chem. Phys. 10 (2008) 1457.

[46] E. Naudin, H.A. Ho, S. Branchaud, L. Breau, D. Bélanger, Electrochemical polymerization and characterization of poly(3-(4-fluorophenyl)thiophene) in pure ionic liquids, J. Phys. Chem. B. 106 (2002) 10585–10593.

[47] N.A. Kotov, Carbon sheet solutions, Nature. 442 (2006) 254–255.

[48] A.K. Geim, K.S. Novoselov, The rise of graphene, Nat. Mater. 6 (2007) 183–191.

[49] W. Ren, H.-M. Cheng, The global growth of graphene, Nat. Nanotechnol. 9 (2014) 726–730.

[50] T. Kobayashi, M. Bando, N. Kimura, K. Shimizu, K. Kadono, N. Umezu, K. Miyahara, S. Hayazaki, S. Nagai, Y. Mizuguchi, Y. Murakami, D. Hobara, Production of a 100-m-long high-quality graphene transparent conductive film by roll-to-roll chemical vapor deposition and transfer process, Appl. Phys. Lett. 102 (2013) 023112.

[51] C. Berger, Z. Song, X. Li, X. Wu, N. Brown, C. Naud, D. Mayou, T. Li, J. Hass, A.N. Marchenkov, E.H. Conrad, P.N. First, W.A. de Heer, Electronic Confinement and Coherence in Patterned Epitaxial Graphene, Science 312 (2006) 1191–1196.

[52] K.S. Novoselov, A.K. Geim, S. V Morozov, D. Jiang, Y. Zhang, S. V Dubonos, I. V Grigorieva, A.A. Firsov, Electric field effect in atomically thin carbon films, Science 306 (2004) 666–669.

[53] N.A. Kotov, I. Dekany, J.H. Fendler, Ultrathin Graphite Oxide-Polyelectrolyte Composites Prepared by Self-Assembly: Transition Between Conductive and Non-Conductive States, Adv. Mater. 8 (1996) 637–641.

[54] Y. Hernandez, V. Nicolosi, M. Lotya, F.M. Blighe, Z. Sun, S. De, I.T. McGovern, B. Holland, M. Byrne, Y.K. Gun'ko, J.J. Boland, P. Niraj, G. Duesberg, S. Krishnamurthy, R. Goodhue, J. Hutchison, V. Scardaci, A.C. Ferrari, J.N. Coleman, High-yield production of graphene by liquid-phase exfoliation of graphite, Nat. Nanotechnol. 3 (2008) 563–568.

[55] R. Bari, G. Tamas, F. Irin, A.J.A. Aquino, M.J. Green, E.L. Quitevis, Direct exfoliation of graphene in ionic liquids with aromatic groups, Colloids Surfaces A Physicochem. Eng. Asp. 463 (2014) 63–69.

[56] X. Li, G. Zhang, X. Bai, X. Sun, X. Wang, E. Wang, H. Dai, Highly conducting graphene sheets and Langmuir-Blodgett films, Nat. Nanotechnol. 3 (2008) 538–542.

[57] M. Lotya, Y. Hernandez, P.J. King, R.J. Smith, V. Nicolosi, L.S. Karlsson, F.M. Blighe, S. De, Z. Wang, I.T. McGovern, G.S. Duesberg, J.N. Coleman, Liquid Phase Production of Graphene by Exfoliation of Graphite in Surfactant/Water Solutions, J. Am. Chem. Soc. 131 (2009) 3611–3620.

[58] M. Lotya, P.J. King, U. Khan, S. De, J.N. Coleman, High-Concentration, Surfactant- Stabilized Graphene Dispersions, ACS Nano. 4 (2010) 3155–3162.

[59] D. Parviz, S. Das, H.S.T. Ahmed, F. Irin, S. Bhattacharia, M.J. Green, Dispersions of non-covalently functionalized graphene with minimal stabilizer, ACS Nano. 6 (2012) 8857–8867.

[60] A. Viinikanoja, J. Kauppila, P. Damlin, E. Mäkilä, J. Leiro, T. Ääritalo, J. Lukkari, Interactions between graphene sheets and ionic molecules used for the shear-assisted exfoliation of natural graphite, Carbon 68 (2014) 195–209.

[61] J.W. Lee, J.U. Lee, J.W. Jo, S. Bae, K.T. Kim, W.H. Jo, In-situ preparation of graphene/poly(styrenesulfonic acid-graft-polyaniline) nanocomposite via direct exfoliation of graphite for supercapacitor application, Carbon 105 (2016) 191–198.

[62] H. Xu, K.S. Suslick, Sonochemical Preparation of Functionalized Graphenes, J. Am. Chem. Soc. 133 (2011) 9148–9151.

[63] T. Skaltsas, G. Mountrichas, S. Zhao, H. Shinohara, N. Tagmatarchis, S. Pispas, Single-Step Functionalization and Exfoliation of Graphene with Polymers under Mild Conditions, Chem. - A Eur. J. 21 (2015) 18841–18846.

[64] J. Lu, J. Yang, J. Wang, A. Lim, S. Wang, K.P. Loh, One-Pot Synthesis of Fluorescent Carbon Graphene by the Exfoliation of Graphite in Ionic Liquids, ACS

Nano. 3 (2009) 2367–2375.

[65] I. Tsai, J. Cao, L. Le Fevre, B. Wang, R. Todd, R.A.W. Dryfe, A.J. Forsyth, Graphene-enhanced electrodes for scalable supercapacitors, Electrochim. Acta. 257 (2017) 372–379.

[66] J. Liu, M. Notarianni, G. Will, V.T. Tiong, H. Wang, N. Motta, Electrochemically exfoliated graphene for electrode films: Effect of graphene flake thickness on the sheet resistance and capacitive properties, Langmuir. 29 (2013) 13307–13314.

[67] K. Parvez, Z.S. Wu, R. Li, X. Liu, R. Graf, X. Feng, K. Müllen, Exfoliation of graphite into graphene in aqueous solutions of inorganic salts, J. Am. Chem. Soc. 136 (2014) 6083–6091.

[68] C.Y. Su, A.Y. Lu, Y. Xu, F.R. Chen, A.N. Khlobystov, L.J. Li, High-quality thin graphene films from fast electrochemical exfoliation, ACS Nano. 5 (2011) 2332–2339.

[69] K. Parvez, R. Li, S.R. Puniredd, Y. Hernandez, F. Hinkel, S. Wang, X. Feng, K. Müllen, Electrochemically exfoliated graphene as solution-processable, highly conductive electrodes for organic electronics, ACS Nano. 7 (2013) 3598–3606.

[70] M. Sevilla, G.A. Ferrero, A.B. Fuertes, Aqueous Dispersions of Graphene from Electrochemically Exfoliated Graphite, Chem. - A Eur. J. 22 (2016) 17351–17358.

[71] S. Yang, S. Brüller, Z.-S. Wu, Z. Liu, K. Parvez, R. Dong, F. Richard, P. Samorì, X. Feng, K. Müllen, Organic Radical-Assisted Electrochemical Exfoliation for the Scalable Production of High-Quality Graphene, J. Am. Chem. Soc. 137 (2015) 13927–13932.

[72] A. Ejigu, I.A. Kinloch, R.A.W. Dryfe, Single Stage Simultaneous Electrochemical Exfoliation and Functionalization of Graphene, ACS Appl. Mater. Interfaces. 9 (2017) 710–721.

[73] N. Liu, F. Luo, H. Wu, Y. Liu, C. Zhang, J. Chen, B.N. Liu, F. Luo, H. Wu, Y. Liu, C. Zhang, J. Chen, One-step ionic-liquid-assisted electrochemical synthesis of ionic-liquid-functionalized graphene sheets directly from graphite, Adv. Funct. Mater. 18 (2008) 1518–1525.

[74] A.P. Saxena, M. Deepa, A.G. Joshi, S. Bhandari, A.K. Srivastava, Poly(3,4-ethylenedioxythiophene)-Ionic Liquid Functionalized Graphene/Reduced Graphene Oxide Nanostructures: Improved Conduction and Electrochromism, ACS Appl. Mater. Interfaces. 3 (2011) 1115–1126.

[75] B.C. Brodie, On the Atomic Weight of Graphite, Philos. Trans. R. Soc. London. 149 (1859) 249–259.

[76] L. Staudenmaier, Verfahren zur Darstellung der Graphitsäure, Berichte Der Dtsch. Chem. Gesellschaft. 31 (1898) 1481–1487.

[77] W.S. Hummers, R.E. Offeman, Preparation of Graphitic Oxide, J. Am. Chem. Soc. 208 (1958) 1937.

[78] M. Zhou, Y. Wang, Y. Zhai, J. Zhai, W. Ren, F. Wang, S. Dong, Controlled Synthesis of Large-Area and Patterned Electrochemically Reduced Graphene Oxide Films, Chem. - A Eur. J. 15 (2009) 6116–6120.

[79] H.C. Schniepp, J.-L. Li, M.J. McAllister, H. Sai, M. Herrera-Alonso, D.H. Adamson, R.K. Prud'homme, R. Car, D. a Saville, I. a Aksay, Functionalized single graphene sheets derived from splitting graphite oxide, J. Phys. Chem. B Lett. 110 (2006) 8535–8539.

[80] S. Stankovich, D. a. Dikin, R.D. Piner, K. a. Kohlhaas, A. Kleinhammes, Y. Jia, Y. Wu, S.T. Nguyen, R.S. Ruoff, Synthesis of graphene-based nanosheets via chemical reduction of exfoliated graphite oxide, Carbon 45 (2007) 1558–1565.

[81] H. Wang, J.T. Robinson, X. Li, H. Dai, Solvothermal Reduction of Chemically Exfoliated Graphene Sheets, J. Am. Chem. Soc. 131 (2009) 9910–9911.

[82] J.R. Lomeda, C.D. Doyle, D. V. Kosynkin, W.-F. Hwang, J.M. Tour, Diazonium Functionalization of Surfactant-Wrapped Chemically Converted Graphene Sheets, J. Am. Chem. Soc. 130 (2008) 16201–16206.

[83] S. Stankovich, R.D. Piner, S.B.T. Nguyen, R.S. Ruoff, Synthesis and exfoliation of isocyanate-treated graphene oxide nanoplatelets, Carbon 44 (2006) 3342–3347.

[84] S. Stankovich, D. a Dikin, G.H.B. Dommett, K.M. Kohlhaas, E.J. Zimney, E. a Stach, R.D. Piner, S.T. Nguyen, R.S. Ruoff, Graphene-based composite materials., Nat. Lett. 442 (2006) 282–286.

[85] S. Wang, P.-J. Chia, L.-L. Chua, L.-H. Zhao, R.-Q. Png, S. Sivaramakrishnan, M. Zhou, R.G.-S. Goh, R.H. Friend, A.T.-S. Wee, P.K.-H. Ho, Band-like Transport in Surface-Functionalized Highly Solution-Processable Graphene Nanosheets, Adv. Mater. 20 (2008) 3440–3446.

[86] S. Park, D.A. Dikin, S.T. Nguyen, R.S. Ruoff, Graphene Oxide Sheets Chemically Cross-Linked by Polyallylamine, J. Phys. Chem. C. 113 (2009) 15801–15804.

[87] Y. Yang, J. Wang, J. Zhang, J. Liu, X. Yang, H. Zhao, Exfoliated Graphite Oxide Decorated by PDMAEMA Chains and Polymer Particles, Langmuir. 25 (2009) 11808–11814.

[88] D. Yu, Y. Yang, M. Durstock, J.-B. Baek, L. Dai, Soluble P3HT-Grafted Graphene for Efficient Bilayer−Heterojunction Photovoltaic Devices, ACS Nano. 4 (2010) 5633–5640.

[89] N. Naidek, A.J.G. Zarbin, E.S. Orth, Covalently linked nanocomposites of polypyrrole with graphene: Strategic design toward optimized properties, J. Polym. Sci. Part A Polym. Chem. 56 (2018) 579–588.

[90] J.I. Paredes, S. Villar-Rodil, A. Martínez-Alonso, J.M.D. Tascón, Graphene oxide dispersions in organic solvents, Langmuir. 24 (2008) 10560–10564.

[91] S. Park, J. An, I. Jung, R.D. Piner, S.J. An, X. Li, A. Velamakanni, R.S. Ruoff, Colloidal Suspensions of Highly Reduced Graphene Oxide in a Wide Variety of Organic Solvents, Nano Lett. 9 (2009) 1593–1597.

[92] S. Stankovich, R.D. Piner, X. Chen, N. Wu, S.T. Nguyen, R.S. Ruoff, Stable aqueous dispersions of graphitic nanoplatelets via the reduction of exfoliated graphite oxide in the presence of poly(sodium 4-styrenesulfonate), J. Mater. Chem. 16 (2006) 155–158.

[93] H. Chang, G. Wang, A. Yang, X. Tao, X. Liu, Y. Shen, Z. Zheng, A transparent, flexible, low-temperature, and solution-processible graphene composite electrode, Adv. Funct. Mater. 20 (2010) 2893–2902.

[94] S.-Z. Zu, B.-H. Han, Aqueous Dispersion of Graphene Sheets Stabilized by Pluronic Copolymers: Formation of Supramolecular Hydrogel, J. Phys. Chem. C. 113 (2009) 13651–13657.

[95] X. Jin, K. Adpakpang, I. Young Kim, S. Mi Oh, N.-S. Lee, S.-J. Hwang, An Effective Way to Optimize the Functionality of Graphene-Based Nanocomposite: Use of the Colloidal Mixture of Graphene and Inorganic Nanosheets, Sci. Rep. 5

(2015) 11057.

[96] T. Fukushima, a Kosaka, Y. Ishimura, T. Yamamoto, T. Takigawa, N. Ishii, T. Aida, Molecular Ordering of Organic Molten Salts Trigged by Single-Walled Carbon Nanotubes, Science 300 (2003) 2072–2074.

[97] J. Wang, H. Chu, Y. Li, Why Single-Walled Carbon Nanotubes Can Be Dispersed in Imidazolium-Based Ionic Liquids, ACS Nano. 2 (2008) 2540–2546.

[98] B. Zhang, W. Ning, J. Zhang, X. Qiao, J. Zhang, J. He, C. Liu, Stable dispersions of reduced graphene oxide in ionic liquids, J. Mater. Chem. 20 (2010) 5401.

[99] M.. M. Acik, D.R.D.R.. Dreyer, C.W.. C.W. Bielawski, Y.J.. Y.J. Chabal, Impact of Ionic Liquids on the Exfoliation of Graphite Oxide, J. Phys. Chem. C. 116 (2012) 7867–7873.

[100] T. Zhang, P. Liu, C. Sheng, Y. Duan, J. Zhang, A green and facile approach for the synthesis of water-dispersible reduced graphene oxide based on ionic liquids, Chem. Commun. 50 (2014) 2889–2892.

[101] H. Bai, C. Li, G. Shi, Functional Composite Materials Based on Chemically Converted Graphene, Adv. Mater. 23 (2011) 1089–1115.

[102] D. Nguyen, H. Yoon, Recent Advances in Nanostructured Conducting Polymers: from Synthesis to Practical Applications, Polymers 8 (2016) 118.

[103] M. Moussa, Z. Zhao, M.F. El-Kady, H. Liu, A. Michelmore, N. Kawashima, P. Majewski, J. Ma, Free-standing composite hydrogel films for superior volumetric capacitance, J. Mater. Chem. A. 3 (2015) 15668–15674.

[104] C. Karlsson, J. Nicholas, D. Evans, M. Forsyth, M. Strømme, M. Sjödin, P.C. Howlett, C. Pozo-Gonzalo, Stable Deep Doping of Vapor-Phase Polymerized Poly(3,4-ethylenedioxythiophene)/Ionic Liquid Supercapacitors, ChemSusChem. 9 (2016) 2112–2121.

[105] Q. Wu, Y. Xu, Z. Yao, A. Liu, G. Shi, Supercapacitors Based on Flexible Graphene/Polyaniline Nanofiber Composite Films, ACS Nano. 4 (2010) 1963–1970.

[106] Z.-F. Li, H. Zhang, Q. Liu, L. Sun, L. Stanciu, J. Xie, Fabrication of high-surface-area graphene/polyaniline nanocomposites and their application in supercapacitors, ACS Appl. Mater. Interfaces. 5 (2013) 2685–2691.

[107] Y. Ge, C. Wang, K. Shu, C. Zhao, X. Jia, S. Gambhir, G.G. Wallace, A facile approach for fabrication of mechanically strong graphene/polypyrrole films with large areal capacitance for supercapacitor applications, RSC Adv. 5 (2015) 102643–102651.

[108] H. Wang, Q. Hao, X. Yang, L. Lu, X. Wang, Graphene oxide doped polyaniline for supercapacitors, Electrochem. Commun. 11 (2009) 1158–1161.

[109] H. Wang, Q. Hao, X. Yang, L. Lu, X. Wang, A nanostructured graphene/polyaniline hybrid material for supercapacitors, Nanoscale. 2 (2010) 2164–2170.

[110] L. Mao, K. Zhang, H.S. On Chan, J. Wu, Surfactant-stabilized graphene/polyaniline nanofiber composites for high performance supercapacitor electrode, J. Mater. Chem. 22 (2012) 80–85.

[111] J. Zhang, X.S. Zhao, Conducting Polymers Directly Coated on Reduced Graphene Oxide Sheets as High-Performance Supercapacitor Electrodes, J. Phys. Chem. C. 116 (2012) 5420–5426.

[112] C. Vallés, P. Jiménez, E. Muñoz, A.M. Benito, W.K. Maser, Simultaneous Reduction of Graphene Oxide and Polyaniline: Doping-Assisted Formation of a Solid-State Charge-Transfer Complex, J. Phys. Chem. C. 115 (2011) 10468–10474.

[113] Z. Tong, Y. Yang, J. Wang, J. Zhao, B.-L. Su, Y. Li, Layered polyaniline/graphene film from sandwich-structured polyaniline/graphene/polyaniline nanosheets for high-performance pseudosupercapacitors, J. Mater. Chem. A. 2 (2014) 4642–4651.

[114] J. Xu, K. Wang, S.Z. Zu, B.H. Han, Z. Wei, Hierarchical nanocomposites of polyaniline nanowire arrays on graphene oxide sheets with synergistic effect for energy storage, ACS Nano. 4 (2010) 5019–5026.

[115] T. Lindfors, A. Österholm, J. Kauppila, M. Pesonen, Electrochemical reduction of graphene oxide in electrically conducting poly(3,4-ethylenedioxythiophene) composite films, Electrochim. Acta. 110 (2013) 428–436.

[116] Y. Liu, B. Zhang, Q. Xu, Y. Hou, S. Seyedin, S. Qin, G.G. Wallace, S. Beirne, J.M. Razal, J. Chen, Development of Graphene Oxide/Polyaniline Inks for High Performance Flexible Microsupercapacitors via Extrusion Printing, Adv. Funct. Mater. 28 (2018) 1706592.

[117] J. Pedrós, A. Boscá, J. Martínez, S. Ruiz-Gómez, L. Pérez, V. Barranco, F. Calle, Polyaniline nanofiber sponge filled graphene foam as high gravimetric and volumetric capacitance electrode, J. Power Sources. 317 (2016) 35–42.

[118] H. Zhou, G. Han, Y. Xiao, Y. Chang, H.-J. Zhai, Facile preparation of polypyrrole/graphene oxide nanocomposites with large areal capacitance using electrochemical codeposition for supercapacitors, J. Power Sources. 263 (2014) 259–267.

[119] A. Liu, C. Li, H. Bai, G. Shi, Electrochemical Deposition of Polypyrrole/Sulfonated Graphene Composite Films, J. Phys. Chem. C. 114 (2010) 22783–22789.

[120] Y. Yang, C. Wang, B. Yue, S. Gambhir, C.O. Too, G.G. Wallace, Electrochemically synthesized polypyrrole/graphene composite film for lithium batteries, Adv. Energy Mater. 2 (2012) 266–272.

[121] A. Österholm, T. Lindfors, J. Kauppila, P. Damlin, C. Kvarnström, Electrochemical incorporation of graphene oxide into conducting polymer films, Electrochim. Acta. 83 (2012) 463–470.

[122] L. Lu, O. Zhang, J. Xu, Y. Wen, X. Duan, H. Yu, L. Wu, T. Nie, A facile one-step redox route for the synthesis of graphene/poly (3,4-ethylenedioxythiophene) nanocomposite and their applications in biosensing, Sensors Actuators B Chem. 181 (2013) 567–574.

[123] Q. Zhang, Y. Li, Y. Feng, W. Feng, Electropolymerization of graphene oxide/polyaniline composite for high-performance supercapacitor, Electrochim. Acta. 90 (2013) 95–100.

[124] T. Lindfors, R.-M. Latonen, Improved charging/discharging behavior of electropolymerized nanostructured composite films of polyaniline and electrochemically reduced graphene oxide, Carbon 69 (2014) 122–131.

[125] T. Lindfors, Z.A. Boeva, R.-M. Latonen, Electrochemical synthesis of poly(3,4-ethylenedioxythiophene) in aqueous dispersion of high porosity reduced graphene oxide, RSC Adv. 4 (2014) 25279–25286.

[126] M. Deng, X. Yang, M. Silke, W. Qiu, M. Xu, G. Borghs, H. Chen, Electrochemical deposition of polypyrrole/graphene oxide composite on microelectrodes towards tuning the electrochemical properties of neural probes, Sensors Actuators B Chem.

158 (2011) 176–184.

[127] M. Wilamowska, M. Kujawa, M. Michalska, L. Lipińska, A. Lisowska-Oleksiak, Electroactive polymer/graphene oxide nanostructured composites; evidence for direct chemical interactions between PEDOT and GOx, Synth. Met. 220 (2016) 334–346.

[128] T. Lindfors, A. Österholm, J. Kauppila, R.E. Gyurcsányi, Enhanced electron transfer in composite films of reduced graphene oxide and poly(N-methylaniline), Carbon 63 (2013) 588–592.

[129] D. Wang, F. Li, J. Zhao, W. Ren, Z. Chen, J. Tan, Z. Wu, I. Gentle, G.Q. Lu, H. Cheng, Fabrication of Graphene/Polyaniline Composite Paper via In Situ Anodic Electropolymerization for High-Performance Flexible Electrode, ACS Nano. 3 (2009) 1745–1752.

[130] D. Li, M.B. Müller, S. Gilje, R.B. Kaner, G.G. Wallace, Processable aqueous dispersions of graphene nanosheets, Nat. Nanotechnol. 3 (2008) 101–105.

[131] H. Zhou, X. Zhi, H.-J. Zhai, A strategy to boost electrochemical properties of the graphene oxide–poly(3,4-ethylenedioxythiophene) composites for supercapacitor electrodes, J. Mater. Sci. 53 (2018) 5216–5228.

[132] S. Lehtimäki, M. Suominen, P. Damlin, S. Tuukkanen, C. Kvarnström, D. Lupo, Preparation of Supercapacitors on Flexible Substrates with Electrodeposited PEDOT/Graphene Composites, ACS Appl. Mater. Interfaces. 7 (2015) 22137–22147.

[133] A.W. Lang, J.F. Ponder, A.M. Österholm, N.J. Kennard, R.H. Bulloch, J.R. Reynolds, Flexible, aqueous-electrolyte supercapacitors based on water-processable dioxythiophene polymer/carbon nanotube textile electrodes, J. Mater. Chem. A. 5 (2017) 23887–23897.

[134] G.A. Snook, G.Z. Chen, The measurement of specific capacitances of conducting polymers using the quartz crystal microbalance, J. Electroanal. Chem. 612 (2008) 140–146.

[135] M.E. Plonska-Brzezinska, J. Breczko, B. Palys, L. Echegoyen, The Electrochemical Properties of Nanocomposite Films Obtained by Chemical In Situ Polymerization of Aniline and Carbon Nanostructures, ChemPhysChem. 14 (2013) 116–124.

[136] D. Weingarth, A. Foelske-Schmitz, R. Kötz, Cycle versus voltage hold - Which is the better stability test for electrochemical double layer capacitors?, J. Power Sources. 225 (2013) 84–88.

[137] H. Olsson, G. Nyström, M. Strømme, M. Sjödin, L. Nyholm, Cycling stability and self-protective properties of a paper-based polypyrrole energy storage device, Electrochem. Commun. 13 (2011) 869–871.

[138] Z. Wang, P. Tammela, M. Strømme, L. Nyholm, Nanocellulose coupled flexible polypyrrole@graphene oxide composite paper electrodes with high volumetric capacitance, Nanoscale. 7 (2015) 3418–3423.

[139] A. Borenstein, O. Hanna, R. Attias, S. Luski, T. Brousse, D. Aurbach, Carbon-based composite materials for supercapacitor electrodes: a review, J. Mater. Chem. A. 5 (2017) 12653–12672.

[140] V. Khomenko, E. Frackowiak, F. Béguin, Determination of the specific capacitance of conducting polymer/nanotubes composite electrodes using different cell configurations, Electrochim. Acta. 50 (2005) 2499–2506.

[141] E. Frackowiak, V. Khomenko, K. Jurewicz, K. Lota, F. Béguin, Supercapacitors based on conducting polymers/nanotubes composites, J. Power Sources. 153 (2006) 413–418.

[142] Z. Wang, D.O. Carlsson, P. Tammela, K. Hua, P. Zhang, L. Nyholm, M. Strømme, Surface Modified Nanocellulose Fibers Yield Conducting Polymer-Based Flexible Supercapacitors with Enhanced Capacitances, ACS Nano. 9 (2015) 7563–7571.

[143] T. Lindfors, Potential Cycling Stability of Composite Films of Graphene Derivatives and Poly(3,4-ethylenedioxythiophene), Electroanalysis. 27 (2015) 727–732.

[144] F. Wang, Y.H. Lai, N.M. Kocherginsky, Y.Y. Kosteski, The first fully characterized 1,3-polyazulene: High electrical conductivity resulting from cation radicals and polycations generated upon protonation, Org. Lett. 5 (2003) 995–998.

[145] G. Nie, T. Cai, S. Zhang, J. Hou, J. Xu, X. Han, Low potential electrosyntheses of high quality freestanding polyazulene films, Mater. Lett. 61 (2007) 3079–3082.

[146] E. Grodzka, K. Winkler, B.M. Esteban, C. Kvarnstrom, Capacitance properties of electrochemically deposited polyazulene films, Electrochim. Acta. 55 (2010) 970–978.

[147] N. He, R.E. Gyurcsányi, T. Lindfors, Electropolymerized hydrophobic polyazulene as solid-contacts in potassium-selective electrodes, Analyst. 141 (2016) 2990–2997.

[148] M. Zagorska, A. Pron, S. Lefrant, Spectroelectrochemistry and Spectroscopy of Conducting Polymers, in: H.S. Nalwa (Ed.), Handb. Org. Conduct. Mol. Polym., 3rd ed., Wiley, Chichester, 1997: pp. 183–218.

[149] C. Kvarnström, A. Ivaska, H. Neugebauer, Infrared Spectroelectrochemistry on Conducting Polymers and Fullerenes, in: H.S. Nalwa (Ed.), Adv. Funct. Mol. Polym., 2nd editio, Gordon & Breach Science Publishers, 2001: pp. 139–170.

[150] G. Nöll, C. Lambert, M. Lynch, M. Porsch, J. Daub, Electronic Structure and Properties of Poly- and Oligoazulenes, J. Phys. Chem. C. 112 (2008) 2156–2164.

[151] G. Horowitz, A. Yassar, H.J. von Bardeleben, ESR and optical spectroscopy evidence for a chain-length dependence of the charged states of thiophene oligomers. Extrapolation to polythiophene, Synth. Met. 62 (1994) 245–252.

[152] A. Österholm, A. Petr, C. Kvarnström, A. Ivaska, L. Dunsch, The nature of the charge carriers in polyazulene as studied by in situ electron spin resonance-UV-visible-near-infrared spectroscopy, J. Phys. Chem. B. 112 (2008) 14149–14157.

[153] H. Neugebauer, Infrared signatures of positive and negative charge carriers in conjugated polymers with low band gaps, J. Electroanal. Chem. 563 (2004) 153–159.

[154] A. Kellenberger, E. Dmitrieva, L. Dunsch, Structure Dependence of Charged States in “Linear” Polyaniline as Studied by In Situ ATR-FTIR Spectroelectrochemistry, J. Phys. Chem. B. 116 (2012) 4377–4385.

[155] B. Meana-Esteban, C. Lete, C. Kvarnström, A. Ivaska, Raman and in situ FTIR-ATR characterization of polyazulene films and its derivate, J. Phys. Chem. B. 110 (2006) 23343–23350.

[156] R.-M. Latonen, B. Meana Esteban, C. Kvarnström, A. Ivaska, Electrochemical polymerization and characterization of a poly(azulene)-TiO2 nanoparticle composite film, J. Appl. Electrochem. 39 (2009) 653–661.

[157] R.-M. Latonen, A. Österholm, C. Kvarnström, A. Ivaska, Electrochemical and

Spectroelectrochemical Study of Polyazulene/BBL-PEO Donor–Acceptor Composite Layers, J. Phys. Chem. C. 116 (2012) 23793–23802.

[158] G. Milczarek, O. Inganas, Renewable Cathode Materials from Biopolymer/Conjugated Polymer Interpenetrating Networks, Science 335 (2012) 1468–1471.

[159] F.N. Ajjan, M.J. Jafari, T. Rębiś, T. Ederth, O. Inganäs, Spectroelectrochemical investigation of redox states in a polypyrrole/lignin composite electrode material, J. Mater. Chem. A. 3 (2015) 12927–12937.

[160] F.W. Richey, B. Dyatkin, Y. Gogotsi, Y.A. Elabd, Ion dynamics in porous carbon electrodes in supercapacitors using in situ infrared spectroelectrochemistry, J. Am. Chem. Soc. 135 (2013) 12818–12826.

[161] M. Hirata, T. Gotou, S. Horiuchi, M. Fujiwara, M. Ohba, Thin-film particles of graphite oxide 1: High-yield synthesis and flexibility of the particles, Carbon 42 (2004) 2929–2937.

[162] P. Nockemann, K. Binnemans, B. Thijs, T.N. Parac-Vogt, K. Merz, A.-V. Mudring, P.C. Menon, R.N. Rajesh, G. Cordoyiannis, J. Thoen, J. Leys, C. Glorieux, Temperature-Driven Mixing-Demixing Behavior of Binary Mixtures of the Ionic Liquid Choline Bis(trifluoromethylsulfonyl)imide and Water, J. Phys. Chem. B. 113 (2009) 1429–1437.

[163] L. Cammarata, S.G. Kazarian, P. a. Salter, T. Welton, Molecular states of water in room temperature ionic liquids, Phys. Chem. Chem. Phys. 3 (2001) 5192–5200.

[164] J. Kauppila, P. Kunnas, P. Damlin, A. Viinikanoja, C. Kvarnström, Electrochemical reduction of graphene oxide films in aqueous and organic solutions, Electrochim. Acta. 89 (2013) 84–89.

[165] G.K. Ramesha, S. Sampath, Electrochemical Reduction of Oriented Graphene Oxide Films: An in Situ Raman Spectroelectrochemical Study, J. Phys. Chem. C. 113 (2009) 7985–7989.

[166] K.R. Seddon, A. Stark, M.-J. Torres, Influence of chloride, water, and organic solvents on the physical properties of ionic liquids, Pure Appl. Chem. 72 (2000) 2275–2287.

[167] A.M. Dimiev, L.B. Alemany, J.M. Tour, Graphene oxide. Origin of acidity, its instability in water, and a new dynamic structural model., ACS Nano. 7 (2013) 576–588.

[168] A. Österholm, B. Meana-Esteban, C. Kvarnström, A. Ivaska, In situ Resonance Raman Spectroscopy of Polyazulene on Aluminum, J. Phys. Chem. B. 112 (2008) 6331–6337.

[169] A.J.L. Costa, M.R.C. Soromenho, K. Shimizu, I.M. Marrucho, J.M.S.S. Esperanca, J.N.C. Lopes, L.P.N. Rebelo, Density, thermal expansion and viscosity of cholinium-derived ionic liquids, ChemPhysChem. 13 (2012) 1902–1909.

[170] M. Dietrich, J. Heinze, G. Heywang, F. Jonas, Electrochemical and spectroscopic characterization of polyalkylenedioxythiophenes, J. Electroanal. Chem. 369 (1994) 87–92.

Annales Universitatis Turkuensis

UNIVERSITY OF TURKU

Grano Oy, Turku, Finland 2019

ISBN 978-951-29-7554-9 (PRINT)
ISBN 978-951-29-7555-6 (PDF)
ISSN 0082-7002 (Print)
ISSN 2343-3175 (Online)